A New Look at the Problem of Tropical Cyclones in Vertical Shear Flow: Vortex Resiliency

PAUL D. REASOR AND MICHAEL T. MONTGOMERY

Department of Atmospheric Science, Colorado State University, Fort Collins, Colorado

LEWIS D. GRASSO

CIRA/Colorado State University, Fort Collins, Colorado

(Manuscript received 8 April 2003, in final form 26 June 2003)

ABSTRACT

A new paradigm for the resiliency of tropical cyclone (TC) vortices in vertical shear flow is presented. To elucidate the basic dynamics, the authors follow previous work and consider initially barotropic vortices on an f plane. It is argued that the diabatically driven secondary circulation of the TC is not *directly* responsible for maintaining the vertical alignment of the vortex. Rather, an inviscid damping mechanism intrinsic to the dry adiabatic dynamics of the TC vortex suppresses departures from the upright state.

Recent work has demonstrated that tilted quasigeostrophic vortices consisting of a core of positive vorticity surrounded by a skirt of lesser positive vorticity align through projection of the tilt asymmetry onto vortex Rossby waves (VRWs) and their subsequent damping (VRW damping). This work is extended here to the finite Rossby number (Ro) regime characteristic of real TCs. It is shown that the VRW damping mechanism provides a direct means of reducing the tilt of intense cyclonic vortices (Ro > 1) in unidirectional vertical shear. Moreover, intense TC-like, but initially barotropic, vortices are shown to be much more resilient to vertical shearing than previously believed. For initially upright, observationally based TC-like vortices in vertical shear, the existence of a ''downshear-left'' tilt equilibrium is demonstrated when the VRW damping is nonnegligible.

On the basis of these findings, the axisymmetric component of the diabatically driven secondary circulation is argued to contribute indirectly to vortex resiliency against shear by increasing Ro and enhancing the radial gradient of azimuthal-mean potential vorticity. This, in addition to the reduction of static stability in moist ascent regions, increases the efficiency of the VRW damping mechanism.

1. Introduction

The impact of environmental vertical shear on the formation and intensification of tropical cyclones (TCs) has long been recognized as a largely negative one, severely inhibiting their formation when above a threshold of approximately 12.5–15 m s^{-1} in the 850–200-mb layer (Zehr 1992) and weakening or limiting the development of mature storms (Gray 1968; DeMaria 1996; Frank and Ritchie 2001). The error in TC intensity prediction using statistical models (DeMaria and Kaplan 1999) and operational dynamical models (Kurihara et al. 1998) generally increases when vertical shear is a factor. The error of the dynamical models is believed in part due to deficiencies in the prediction of vertical shear in the vicinity of the TC and also from inadequate representation of the interaction of the TC with the vertical shear flow. Regarding the latter issue, studies of TCs in vertical shear have sought to define what is ''adequate.'' One of the principal questions is: Do the details of cumulus convection determine whether a given storm shears apart or remains vertically aligned, or can the effect of convection be meaningfully parameterized and still yield a reasonably accurate forecast? Even more basic, what *is* the role of convection in the vertical alignment of TCs in shear?

When examining the causes of TC resiliency in vertical shear, we believe the hypothesis that moist processes (e.g., deep cumulus convection) supersede mechanisms intrinsic to the dry ''adiabatic'' dynamics is without merit. While it is generally acknowledged that diabatic processes are essential to the maintenance of TCs in both quiescent and vertically sheared environments (Ooyama 1969; Shapiro and Willoughby 1982; Montgomery and Enagonio 1998; Davis and Bosart 2001), we will argue here that without the dry adiabatic mechanisms (modified by the presence of convection) TCs would have little chance of surviving differential advection by the vertical shear flow.

In a comparison of dry and moist numerical simulations of an initially weak vortex embedded in weak

Corresponding author address: Dr. Paul D. Reasor, Dept. of Meteorology, The Florida State University, Tallahassee, FL 32306-4520. E-mail: reasor@met.fsu.edu.

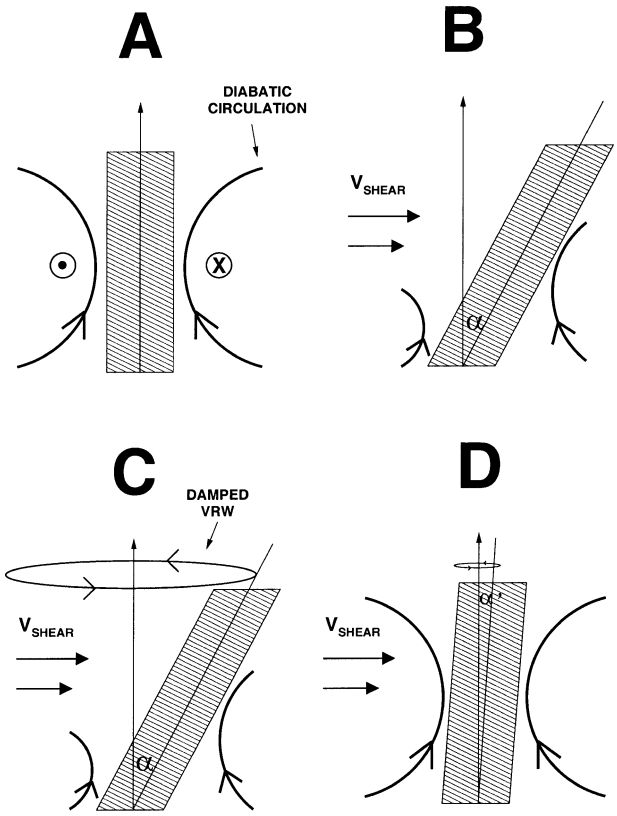

FIG. 1. Schematic of the TC alignment mechanism when the TC vortex is tilted by vertical shear. (a) The primary TC circulation (into and out of the page) is maintained in the presence of frictional drag through stretching of mean TC vorticity by the diabatically driven axisymmetric secondary circulation. (b) Vertical shear causes the TC to tilt (with vertical tilt angle α). Eyewall convection responds by becoming increasingly asymmetric, with a maximum in the downshear quadrant of the storm. The asymmetric component of convection increases at the expense of the symmetric component shown in (a). No longer able to offset the frictional drag, the mean TC weakens. In the absence of an intrinsic mechanism to realign, the TC will shear apart. (c) Recent work has identified an intrinsic alignment mechanism called VRW damping. VRW damping counters differential advection of the TC by the vertical shear flow. (d) For sufficiently strong VRW damping, a quasi-aligned vortex ($\alpha' \ll \alpha$) is possible with a secondary circulation similar to the axisymmetric configuration of (a).

vertical shear, Frank and Ritchie (1999) found that the dry vortex sheared apart, while the intensifying vortex in the model with moist physics remained vertically aligned. Their results affirm the idea that a diabatically driven axisymmetric secondary circulation is needed to stretch vorticity in the TC core, and thus maintain or intensify the vortex against frictional dissipation in the boundary layer (e.g., Shapiro and Willoughby 1982). One should not draw the conclusion, however, that the mechanisms involved in the evolution of the dry vortex become irrelevant once convection is included.

To help illustrate the nature of the physical problem, consider an initially upright TC in a moist, but quiescent environment. Figure 1 illustrates schematically how the TC might evolve once vertical shear strong enough to tilt the vortex is imposed. In Fig. 1a the initial undisturbed TC is shown with cyclonic swirling flow (into and out of the page) and an axisymmetric diabatically driven secondary circulation. When the TC is embedded in westerly environmental vertical shear, the vortex is differentially advected so as to yield a west-to-east tilt with height (Fig. 1b). The asymmetric secondary circulation required to keep the tilted TC quasi-balanced lifts parcels downshear and causes descending motion upshear (Jones 1995). Convection in the TC core will respond asymmetrically, consistent with both observations (e.g., Marks et al. 1992; Reasor et al. 2000; Black et al. 2002; Corbosiero and Molinari 2003; Zehr 2003) and numerical studies (e.g., Wang and Holland 1996; Bender 1997; Frank and Ritchie 1999, 2001). Convection increases downshear and is suppressed upshear at the expense of the axisymmetric component of convection. With the axisymmetric component of the secondary circulation now diminished, the TC becomes more susceptible to differential advection by the vertical shear. Although the secondary circulation and axisymmetrization of convectively generated potential vorticity (PV) anomalies (e.g., Montgomery and Enagonio 1998; Möller and Montgomery 2000) may continue to intensify the symmetric component of the TC, the question remains how to reduce the tilt asymmetry.

Jones (1995; hereafter SJ95) showed that, when a barotropic vortex is tilted by vertical shear, the coupling between upper- and lower-level cyclonic PV anomalies results in cyclonic precession of the vortex. The precession upshear reduces the vortex tilt from what would otherwise occur if the vortex were simply advected by the vertical shear flow. In her benchmark simulation without moist processes using a hurricane-strength (40 m s^{-1}) vortex embedded in 4 m s^{-1} (10 km)$^{-1}$ vertical shear, the vortex did precess, but the vortex tilt *increased* with time. Contrary to the results of SJ95, in a dry adiabatic simulation of a hurricane vortex embedded in approximately 7 m s^{-1} vertical shear through the depth of the troposphere, Wang and Holland (1996) found that the cyclonic portion of the vortex remained upright. The vortex tilted, realigned, and then achieved a quasi-steady tilt ''downshear-left'' over a 72-h period (see their Fig. 4). In a subsequent study, Jones (2000a) examined the role of large-scale asymmetries generated by the vertically penetrating flow of the tilted vortex. She found that the impact of such asymmetries on the vortex tilt is dependent on the radial structure of the initial mean vortex. For the benchmark profile of SJ95, Jones (2000a) showed a case where advection across the vortex core by the large-scale asymmetry appeared to realign the vortex. For a much broader vortex wind profile, the impact of the large-scale asymmetry on the tilt of the vortex core was reduced, yielding an evolution more in line with Wang and Holland (1996). The results of Wang and Holland are supported by the recent numerical study of Frank and Ritchie (2001). In a full-physics

simulation of a hurricane in 5 m s^{-1} vertical shear through the depth of the troposphere, Frank and Ritchie found that the shear had negligible impact on the vortex intensity and vertical tilt out to almost two days after the shear was imposed. Based on the above recent numerical simulations, it is clear that there exists a subtle dependence of the TC-in-shear dynamics on radial vortex profile. Our aim here is to expose the precise nature of this dependence.

A new theory for the alignment of quasigeostrophic (QG) vortices, which separates clearly the mean vortex evolution from the evolution of the tilt asymmetry, has been developed by Reasor and Montgomery (2001; hereafter RM01) and Schecter et al. (2002; hereafter SMR). Although from different perspectives, these studies demonstrate the fundamental role of vortex Rossby waves (VRWs) in the relaxation of tilted vortices to an aligned state. We believe this VRW approach is the key to understanding how a TC maintains its aligned structure in the presence of vertical shear.

In RM01 a tilted QG vortex with overlapping upper- and lower-level PV cores was decomposed into an azimuthal mean vortex and small, but finite, tilt perturbation. The subsequent evolution of the vortex tilt perturbation was captured by a linear VRW mechanism. At small values of the ratio of horizontal vortex scale to Rossby deformation radius the vortex precesses through the projection of vortex tilt onto a near-discrete VRW, or ''quasi mode'' (Rivest and Farrell 1992; Schecter et al. 2000). By ''discrete'' we mean the VRW is characterized by a single phase speed and propagates azimuthally without change in radial structure [e.g., an ''edge'' wave on a Rankine vortex (Lamb 1932, 230–231)]. Formally, the evolution of the quasi mode may be described as the superposition of continuum modes, similar to a disturbance in rectilinear shear flow (Case 1960). But unlike simple sheared disturbances whose spectral distribution is broad, the quasi mode is characterized by a dominant eigenfrequency, and thus behaves much like a discrete eigenmode of the linearized system. A vortex supporting a quasi mode will precess cyclonically, as depicted in Fig. 1c. The continuum modes that compose the quasi mode destructively interact, leading to the decay of the quasi mode and hence the vortex tilt (Fig. 1d). In SMR the vortex tilt was viewed instead as a discrete VRW interacting with the vortex circulation. For monotonically decreasing vorticity profiles the discrete VRW (i.e., the tilt) is inviscidly damped through a resonance with the ambient flow rotation frequency at a critical radius where PV is redistributed within a ''cat's eye.'' This means of vortex alignment is termed ''resonant damping.'' The resonantly damped discrete VRW is mathematically equivalent to the quasi mode. With the vortex in a quasi-aligned state, the convection, and hence the diabatically driven secondary circulation, once again approaches axisymmetry.

To examine the resiliency of mature TCs in hostile environments such as vertically sheared flow, we extend here the QG VRW alignment theory to the finite Rossby number regime with vertical shear forcing. We argue that the strengthening and structural modification of the mean vortex by the axisymmetric component of the diabatically driven secondary circulation increase the decay rate of the quasi mode (i.e., the tilt). Thus, while diabatic processes do not supersede the dry adiabatic mechanisms in regards to vortex alignment, we believe they augment the efficiency of the VRW damping mechanism in reducing the tilt.

To demonstrate the dependence of the VRW damping mechanism on vortex strength and structure we use a primitive equation (PE) model in its fully nonlinear, compressible, nonhydrostatic form, as well as a simplified hydrostatic Boussinesq version linearized about a circular vortex in gradient balance. Since our primary aim here is to explain how the tilt of the cyclonic portion of a TC in shear is reduced, we believe it is sufficient to consider initially barotropic cyclonic vortices, as in SJ95. The impact of baroclinic mean vortex structure on the alignment dynamics is reserved for future study. In situations where the vertical shear is confined primarily to the upper troposphere, the downshear advection of the outflow anticyclone found in mature storms may need to be taken into consideration (e.g., Wu and Emanuel 1993; Flatau et al. 1994; Wang and Holland 1996; Corbosiero and Molinari 2003). The influence of the outflow anticyclone is not, in our opinion, well understood, and we believe it is worthy of future study.

The outline of the paper is as follows. Section 2 describes the three numerical models used in this study: the first model is a linearized PE model designed to take advantage of the near-circular symmetry of the problem and our assumption of simple vortex tilts and vertical shear profiles. To elucidate the balanced nature of the tilted vortex evolution we also employ a linearized version of the ''Asymmetric Balance'' (AB) model (Shapiro and Montgomery 1993; McWilliams et al. 2003). Finally, in order to broadly identify the alignment regime boundary, the dry dynamical core of the nonlinear Colorado State University–Regional Atmospheric Modeling System (CSU–RAMS) model (Pielke et al. 1992) is utilized. Section 3 examines the free alignment of broadly distributed vortices at finite Rossby number. Section 4 proposes a new heuristic model for understanding the linearized dynamics of the TC in shear problem. The simple model based on the VRW damping mechanism predicts a downshear-left tilt equilibrium for vortex profiles characteristic of observed TCs. Fully nonlinear numerical simulations are then utilized in section 5 to further our understanding of how TCs maintain their aligned structures in strong shear ($>$10 m s^{-1} over the vortex depth) in the absence of convection. Both idealized and observationally based radial profiles of TC tangential velocity are considered. Implications of these results are discussed in section 6.

2. Numerical models

a. Linear PE model

To develop our basic model of the TC in shear we employ a Boussinesq PE model on an f plane, bounded vertically by rigid lids. The model is formulated in a cylindrical coordinate system (r, λ, z), where z is the pseudoheight vertical coordinate (Hoskins and Bretherton 1972). Consistent with our emphasis on small but finite amplitude departures from vertical alignment, the governing equations are linearized about a circular (mean) vortex in gradient and hydrostatic balance. The mean vortex and hydrostatic perturbation (i.e., the tilt) are then decomposed into barotropic and internal baroclinic modes. As even the linear dynamics at finite Rossby number will be shown to exhibit a rich dynamical structure, we focus here on the simplest case of an initially barotropic vortex. Consistent with hurricane observations (e.g., Hawkins and Rubsam 1968) and recent numerical studies (Rotunno and Emanuel 1987; Möller and Montgomery 2000; RM01; SMR; Schecter and Montgomery 2003) we employ isothermal (constant potential temperature) boundary conditions on the top and bottom of the vortex. Under the Boussinesq approximation, the vertical structure of the modes comprising the geopotential is then given by $\cos(m\pi z/H)$, where m is the vertical mode number and H is the physical depth of the vortex.[1]

The perturbation is Fourier decomposed in azimuth. The prognostic equations for each vertical and azimuthal mode, referred to here as the equivalent barotropic system, are

$$\left(\frac{\partial}{\partial t} + in\overline{\Omega}\right)\hat{u}_{mn}(r, t) - \overline{\xi}\hat{v}_{mn} + \frac{\partial\hat{\phi}_{mn}}{\partial r} = -\alpha(r)\hat{u}_{mn} + F_{u,s}, \tag{1}$$

$$\left(\frac{\partial}{\partial t} + in\overline{\Omega}\right)\hat{v}_{mn}(r, t) + \overline{\eta}\hat{u}_{mn} + \frac{in}{r}\hat{\phi}_{mn} = -\alpha(r)\hat{v}_{mn} + F_{v,s}, \tag{2}$$

$$\left(\frac{\partial}{\partial t} + in\overline{\Omega}\right)\hat{\phi}_{mn}(r, t) + c_m^2\left[\frac{1}{r}\frac{\partial}{\partial r}(r\hat{u}_{mn}) + \frac{in\hat{v}_{mn}}{r}\right] = -\alpha(r)\hat{\phi}_{mn} + F_{\phi,s}, \tag{3}$$

where $\hat{u}_{mn}$, $\hat{v}_{mn}$, and $\hat{\phi}_{mn}$ are the radial velocity, tangential velocity, and geopotential Fourier amplitudes, respectively, for vertical mode m and azimuthal wavenumber n. The azimuthal mean vortex quantities, $\overline{\Omega} = \overline{v}/r$, $\xi = f + 2\overline{\Omega}$, and $\overline{\eta} = f + \overline{\zeta}$, are the angular velocity, modified Coriolis parameter, and absolute vertical vorticity, respectively. Here $\overline{\zeta} = r^{-1}d(r\overline{v})/dr$ is the relative vorticity and f is the constant Coriolis parameter. The internal gravity wave phase speed $c_m = NH/m\pi$, where N is the Brunt–Väisälä frequency and is assumed constant. The first term on the rhs of each equation represents Rayleigh damping within a sponge ring of the form

$$\alpha(r) = \alpha_o \sin^2\left[\frac{\pi(r - r_1)}{r_2 - r_1}\right], \qquad r > r_1, \tag{4}$$

where $r_1 = 2000$ km, $r_2 = 4000$ km, and α_o is a damping rate based on the time it takes a gravity wave to pass through the sponge ring. The second term on the rhs of Eqs. (1)–(3) is a linearized forcing term associated with an imposed vertical shear flow that is assumed weak compared to the basic state swirling flow. The explicit shear forcing terms are given in section 2c.

The system of equations (1)–(3) is discretized radially using centered second-order finite differences on the stencil described in Flatau and Stevens (1989) and Montgomery and Lu (1997). The system is integrated in time using a fourth-order Runge–Kutta time-stepping scheme with a time step less than the maximum value implied by the Courant–Freidrichs–Lewy (CFL) condition. The duration of most simulations examined here is $10\tau_e$, where $\tau_e = 2\pi/\overline{\Omega}(L)$ is a circulation period of the mean vortex at $r = L$, the radius of maximum tangential wind (RMW). Unless otherwise stated, a 3000-km outer radius domain with radial grid spacing $\Delta r = 2.5$ km is used.

The mean PV for a barotropic vortex, $\overline{q} = N^2\overline{\eta}$, is prescribed and the associated tangential velocity field is assumed in gradient balance:

$$f\overline{v} + \frac{\overline{v}^2}{r} = \frac{d\overline{\phi}}{dr}. \tag{5}$$

The perturbation PV amplitude of the initial vortex asymmetry derived from Eqs. (1)–(3),

$$\hat{q}_{mn} = N^2\hat{\zeta}_{mn} - \left(\frac{m\pi}{H}\right)^2\overline{\eta}\hat{\phi}_{mn}, \tag{6}$$

is also prescribed. An iterative solution to (6) and the linear barotropic balance equation (e.g., Montgomery and Franklin 1998),

$$\frac{1}{r}\frac{d}{dr}\left(r\frac{d\hat{\phi}_{mn}}{dr}\right) - \frac{n^2}{r^2}\hat{\phi}_{mn} = \frac{1}{r}\frac{d}{dr}\left(r\overline{\xi}\frac{d\hat{\psi}_{mn}}{dr}\right) - \frac{n^2\overline{\eta}}{r^2}\hat{\psi}_{mn} - \frac{n^2}{r}\frac{d\overline{\Omega}}{dr}\hat{\psi}_{mn}, \tag{7}$$

is sought in order to obtain an initially quasi-balanced perturbation asymmetric wind (defined by the nondivergent streamfunction $\hat{\psi}_{mn}$) and geopotential field $\hat{\phi}_{mn}$. The initial condition employed here to represent a tilted vortex therefore projects minimally onto unbalanced gravity wave motions. Our choice to focus on the bal-

[1] Although the isothermal boundary condition formally breaks down on the top of shallow vortices whose depth is small compared to the tropopause height, we will continue to employ it here as a first approximation to the baroclinic vortex problem.

anced wind field is supported by the PE numerical study of SJ95 where the thermal and wind fields of her simulated tilted vortices in vertical shear were found to evolve in a manner consistent with balanced dynamics.

b. Linear AB model

The balanced nature of the vortex alignment mechanism discussed here is clarified through use of the asymmetric balance (AB) theory (Shapiro and Montgomery 1993). The AB theory has been successfully applied in previous idealized studies of both TC track and intensity change (Montgomery and Kallenbach 1997; Montgomery et al. 1999; Möller and Montgomery 1999, 2000). In the context of vortices supporting quasi modes, Schecter and Montgomery (2003) found that the AB model yields better agreement with the PE model when derived following the ''PV path'' of McWilliams et al. (2003) than when derived following the ''continuity path'' of Shapiro and Montgomery (1993). We follow the former approach here and also find improved agreement with the PE model throughout the vortex alignment phase space characteristic of TC-like vortices. Following the derivation described above for the PE system, a prognostic equation for the perturbation geopotential can be derived for the linear equivalent barotropic AB model:

$$\left(\frac{\partial}{\partial t} + in\overline{\Omega}\right)\left\{\frac{\overline{\eta}\overline{\xi}}{r}\frac{\partial}{\partial r}\left(\frac{r}{\overline{\eta}\overline{\xi}}\frac{\partial\hat{\phi}_{mn}}{\partial r}\right) - \left[S(r)\frac{n^2}{r^2} + \frac{1}{l_r^2(r)}\right]\hat{\phi}_{mn}\right\} - \frac{in\overline{\xi}}{r\overline{\eta}}\frac{d\overline{\eta}}{dr}\hat{\phi}_{mn} = F^{\mathrm{AB}}_{\phi,s}, \tag{8}$$

where $\overline{q} = \overline{\eta}N^2$, as in the PE system, $S(r) = (2\overline{\xi} - \overline{\eta})/\overline{\eta}$ ($=1$ for the continuity path), and $l_r^2(r) = (NH/m\pi)^2(\overline{\eta}\overline{\xi})^{-1}$ is the square of the local internal Rossby deformation radius (Reasor 2000). The term $F^{\mathrm{AB}}_{\phi,s}$ on the rhs represents a vertical shear forcing. In the limit of infinitesimally small Rossby number, $\mathrm{Ro} = V_{\max}/fL$, where $V_{\max}$ is the maximum tangential velocity of the vortex, we note that Eq. (8) reduces to the equivalent barotropic QG PV equation used by RM01. The primary difference between the QG and AB prognostic equations is the replacement of the ''global'' deformation radius, $l_{r,G} = NH/m\pi f$, with a radially dependent local one, $l_r(r)$.

c. Linearized vertical shear forcing

A unidirectional vertically sheared zonal flow is included in the linear PE model in section 5 as a time-invariant forcing with vertical structure of the $m = 1$ baroclinic mode. In cylindrical coordinates the radial and azimuthal components of the zonal shear flow $\mathbf{u}_s$ are expressed as

$$u_s = U\cos(\lambda)\cos\left(\frac{\pi z}{H}\right),$$

$$v_s = -U\sin(\lambda)\cos\left(\frac{\pi z}{H}\right), \tag{9}$$

where U is the zonal velocity at $z = 0$. At $z = H$ the zonal velocity is $-U$, so the net mean flow difference over the depth of the vortex is $2U$. Assuming the zonal flow is geostrophically balanced, the geopotential associated with this wind field is

$$\phi_s = -fUr\sin(\lambda)\cos\left(\frac{\pi z}{H}\right). \tag{10}$$

The shear flow will be viewed here as a small perturbation to the mean vortex. Consequently, in the linearization of the primitive equations, products of shear terms and products of shear and vortex perturbation terms are neglected. For $m = 1$ and $n = 1$ the shear forcing terms in Eqs. (1)–(3) are then as follows:

$$F_{u,s} = \frac{1}{2}iU\overline{\Omega}, \qquad F_{v,s} = -\frac{1}{2}U\frac{d\overline{v}}{dr},$$

$$F_{\phi,s} = \frac{1}{2}fU\overline{v}. \tag{11}$$

Since VRWs are an essential element of the vortex alignment theory of RM01 and its extension here to the forced problem, it proves useful later to express the shear forcing in terms of its effect on the evolution of perturbation PV. The linearized PV equation for the PE system with vertical shear forcing is

$$\left(\frac{\partial}{\partial t} + \overline{\Omega}\frac{\partial}{\partial\lambda}\right)q_m(r,\lambda,t) + u_m\frac{d\overline{q}}{dr} = -U\left\{\frac{d\overline{q}}{dr} + \frac{\overline{v}}{l_{r,G}^2}\frac{\overline{q}}{f}\right\}\cos\lambda, \tag{12}$$

or for $n = 1$,

$$\left(\frac{\partial}{\partial t} + i\overline{\Omega}\right)\hat{q}_{m1}(r,t) + \hat{u}_{m1}\frac{d\overline{q}}{dr} = -\frac{1}{2}U\left\{\frac{d\overline{q}}{dr} + \frac{\overline{v}}{l_{r,G}^2}\frac{\overline{q}}{f}\right\} \equiv F_{q,s}. \tag{13}$$

The shear forcing $F_{q,s}$ in the PV equation (13) is related to the shear forcing in the AB equation (8) by $F^{\mathrm{AB}}_{\phi,s} = \overline{\xi}F_{q,s}/N^2$. The first term on the rhs of Eq. (13) is the differential advection of the vortex PV by the vertical shear flow. The second term on the rhs produces effective β gyres resulting from the advection of zonal PV (associated with the zonal vertical shear) by the mean vortex tangential wind. For all of the sheared vortex simulations presented here this latter forcing is found to be negligible, approximately one to two orders of magnitude less than the first forcing term. According to

Vandermeirsh et al. (2002) in a study of the splitting, or shearing apart, of oceanic-like QG vortices by vertical shear flow in a 2½-layer model, the effective β gyres cause the vortex to remain more resilient. The impact of the β gyres increases with decreasing $l_{r,G}$, thus increasing the shear threshold required to split the vortex. In this limit in the fully nonlinear context, where the mean vortex is allowed to evolve, it is actually possible for the vortex to disperse on the background PV field as Rossby waves before shearing apart. Again, the TC cases considered here are typified by relatively large $l_{r,G}$ compared to horizontal vortex scale, and hence the influence of the effective β gyres is minimal.

d. Fully nonlinear, compressible, nonhydrostatic RAMS model

To investigate the modification of the linear results by nonlinear processes we use the dry dynamical core of the Regional Atmospheric Modeling System version 4.29—developed at Colorado State University (Pielke et al. 1992). Details of the model and the system of equations solved are presented in the appendix. The model domain is 8000 km on a horizontal side (grid spacing $\Delta x = \Delta y = 10$ km) and 10 km in the vertical (grid spacing $\Delta z = 1$ km).

3. Vortex alignment at finite Rossby number

a. Initial conditions

For the experiments presented in this section the radial structure of the azimuthal-mean vortex PV takes the Gaussian form

$$\overline{q}(r) = \overline{q}_{\max} e^{-(\sigma r)^2}, \tag{14}$$

where $\overline{q}_{\max}$ is the maximum mean PV and σ is the inverse decay length of the PV profile. This profile was used by RM01 as an approximation to the broad vorticity distributions observed in weak TCs (e.g., Willoughby 1990). Strong TCs are often characterized by relatively sharp radial gradients of vorticity in the eyewall region (Marks et al. 1992; Reasor et al. 2000; Kossin and Eastin 2001), so the Gaussian structure employed here is a less ideal approximation at large Rossby number. Still, mature hurricanes are far from Rankine vortices, with tangential winds outside the vortex core typically decaying like $r^{-0.4}$ to $r^{-0.6}$ (Riehl 1963; Willoughby 1990; Pearce 1993; Shapiro and Montgomery 1993), as opposed to r^{-1} for the Rankine vortex.

The importance of radial vortex structure in the vertical alignment of QG vortices was highlighted by SMR. For both the Gaussian and ''Rankine-with-skirt'' vortices they found that the tilt decay at $L/l_{r,G} < 2$, where here L is taken to be the RMW, is explained by the decay of a quasi mode. For $L/l_{r,G} > 2$ the tilted Rankine-with-skirt vortex still evolves in a manner consistent with a decaying quasi mode. The alignment of the Gaussian vortex in this regime, however, occurs primarily through axisymmetrization by sheared VRWs. The findings of SMR suggest that the alignment dynamics depends subtly on the radial vortex structure. With this caveat in mind, we will continue to use the Gaussian vortex to present the basic alignment theory at finite Rossby number. In section 5 the theory is applied to both non-Gaussian analytic and observationally based radial vortex profiles.

TABLE 1. Summary of primary numerical experiments examining the free alignment and alignment in vertical shear of initially barotropic cyclonic vortices.

Vortex	$V_{\max}$ (m s^{-1})	L (km)	$l_{r,G}$ (km)	Ro	τ_e (h)	Ambient vertical shear (m s^{-1}/ 10 km)
Gaussian	5	200	100–∞	0.25	69.8	0
Gaussian	40	100	154	3.9	4.4	0
Gaussian	40	100	630	6.5	4.4	0
Gaussian	10	100	1230	3.2	17.5	4
Gaussian	40	100	1230	12.7	4.4	4,8
SJ95	40	100	1230	12.7	4.4	0,4
Olivia	52	17	862	68	0.6	0,10

To mimic the simple tilt of a barotropic vortex we follow RM01 and add to the mean PV a perturbation PV of the form

$$q'(r, \lambda, z) = \mathrm{Re}\left[\hat{q}_{11}(r) e^{i\lambda} \cos\left(\frac{\pi z}{H}\right)\right], \tag{15}$$

where Re[ ] denotes the real part. The amplitude of the PV asymmetry representing the vortex tilt is given by

$$\hat{q}_{11}(r) = \tilde{\alpha} \frac{d\overline{q}}{dr}, \tag{16}$$

where $\tilde{\alpha}$ is a constant. We define $\tilde{\alpha} = \alpha \overline{q}_{\max}/(d\overline{q}/dr)_{\max}$, where $(d\overline{q}/dr)_{\max}$ is the maximum mean PV gradient and α is a nondimensional amplitude.

In the free-alignment experiments we let $\alpha = 0.3$. For this value of tilt amplitude RM01 found good agreement between linear and nonlinear QG simulations for all $l_{r,G}$. In the experiments with zonal vertical shear the initial vortex is vertically aligned ($\alpha = 0$) and allowed to develop a tilt through the differential advection of vortex PV by the shear flow. Pertinent details of the primary numerical experiments are summarized in Table 1.

b. Validation of prior QG results

RM01 showed that, for a broadly distributed QG vortex exhibiting small but finite amplitude tilt, the evolution of the vortex is characterized primarily by the ratio, $L/l_{r,G}$. Using the linear AB theory [see Eq. (8)] as a guide to extending the QG results into the finite Rossby number regime, the appropriate ratio is found to be $L/l_r = (L/l_{r,G})(\sqrt{\overline{\eta}\overline{\xi}}/f)$. As the Rossby number is increased from the infinitesimal values of QG theory,

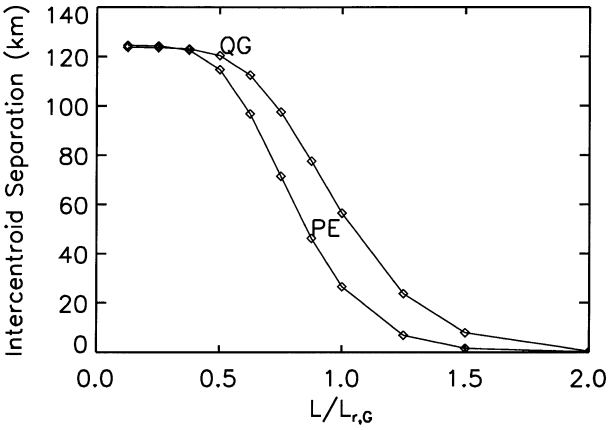

FIG. 2. Vertical alignment of an initially tilted Gaussian vortex. PV intercentroid separation between $z = 0$ and 10 km after $t = 5\tau_e$ as a function of the ratio of RMW to global internal Rossby deformation radius $L/l_{r,G}$. Here, τ_e is a circulation period of the mean vortex at the RMW. The PE results include finite Rossby number effects neglected in the QG formulation. Details of this simulation with $L = 200$ km are listed in Table 1.

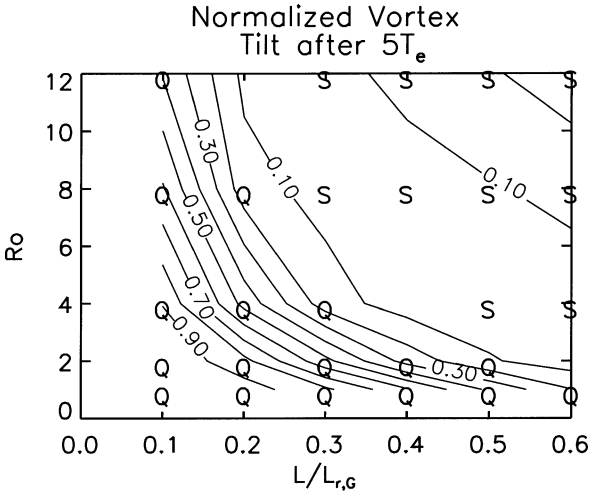

FIG. 3. Azimuthal wavenumber-1 geopotential amplitude $|\hat{\phi}_{11}|$ (normalized by the initial value) at the radius of maximum mean PV gradient of an initially tilted Gaussian vortex after $t = 5\tau_e$, as a function of both Rossby number, Ro, and $L/l_{r,G}$. This quantity will henceforth be used as our canonical measure of vortex tilt. Small contour values indicate near-complete alignment. Vortices clearly supporting a quasi mode are denoted by ''Q,'' while vortices aligning exclusively via sheared VRWs are denoted by ''S.''

L/l_r also increases from its QG value. Schecter and Montgomery (2003) confirmed the hypothesis of RM01 that an increase in L/l_r results in an increased rate of alignment, qualitatively similar to the increase in alignment rate achieved by increasing $L/l_{r,G}$ in the QG theory.

Figure 2 illustrates the modification of the QG results of RM01 by finite Rossby number effects. Shown is the horizontal separation of upper- and lower-level PV centroids after $t = 5\tau_e$ [where $\tau_e = 2\pi/\overline{\Omega}(L)$] as a function of $L/l_{r,G}$ from the linear QG simulations of RM01 and the corresponding linear PE simulations. The vortex in this case has $L = 200$ km and $V_{\max} = 5$ m s^{-1}, yielding Ro = 0.25. The range of deformation radii was obtained by varying the vortex depth. While the inclusion of finite Rossby number effects increases the rate of alignment in the transition regime between precession and complete alignment, the two curves are still in good agreement. At small values of $L/l_{r,G}$ the vortex precesses while slowly aligning through projection of the tilt onto a decaying quasi mode. For $L/l_{r,G} > 2$ the vortex aligns completely over the $5\tau_e$ time period through projection of the tilt onto sheared VRWs. The linear alignment theory of RM01 therefore remains valid at small but finite Rossby number.

For the range of $L/l_{r,G}$ indicated in Fig. 2, SMR demonstrated that the QG decay rate of the vortex tilt is predicted by the theory of resonant damping. An interesting question is whether the resonant damping theory can accurately predict the kind of increases in alignment rate shown in Fig. 2 when the Rossby number is increased. A detailed investigation of the resonant damping theory as it applies to vortex alignment at finite Rossby number is presented by Schecter and Montgomery (2003). For the range of $L/l_{r,G}$ considered here and at order unity Rossby number, they found that Gaussian vortices do indeed support decaying quasi modes. For simple vortex tilts, like those described here, they also found a rapid decay of the vortex tilt over the first τ_e not captured by resonant damping theory. Further details of this initial vortex behavior and a complete examination of the linear alignment phase space typical of TCs are discussed below.

c. Alignment of strong vortices

1) THE LINEAR ALIGNMENT PHASE SPACE

For typical tropical conditions and the gravest vertical modes the global internal deformation radius, $l_{r,G}$ is on the order of 1000 km. For horizontal vortex scales on the order of 100 km, $L/l_{r,G} \sim 0.1$, well within the quasi mode regime according to Fig. 2. If the alignment dynamics at finite Rossby number depends on the *local* deformation radius in a manner similar to the way the QG system depends on $l_{r,G}$, then we might anticipate a transition from alignment via a decaying quasi mode to alignment via sheared VRWs as the Rossby number is increased. We test this hypothesis by mapping out the alignment phase space for a Gaussian vortex of varying Rossby number and typical tropical values of $L/l_{r,G}$. The results using the linearized PE model (1)–(3) are shown in Fig. 3. The geopotential amplitude, $|\hat{\phi}_{11}|$, evaluated at the radius of maximum mean PV gradient is used as a proxy for the tilt of the vortex core. Plotted are values of the tilt after $t = 5\tau_e$, normalized by the initial vortex tilt. The evaluation time is somewhat arbitrary, but given that the environment of a typical TC changes on even shorter time scales, we deemed this time to be meteorologically relevant. For each case shown in Fig. 3 we

have verified the balanced nature of the vortex evolution by comparing the results with the AB theory [Eq. (8)] prediction (not shown). The structure of the phase diagram is reproduced.

It is clear from Fig. 3 that rapid alignment is best achieved by simultaneously increasing the Rossby number and $L/l_{r,G}$. The upper-right portion of the phase space, where the rate of alignment is greatest, is populated by intense, horizontally large but shallow vortices. Conversely, in the lower-left portion of the phase space, where the initial vortex tilt is maintained, vortices are characteristically weak and horizontally small but deep. These results are in qualitative agreement with the sensitivity study of SJ95. She demonstrated that changes in the vortex and environmental parameters that increase the penetration depth, and thus yield stronger vertical coupling between upper- and lower-level PV anomalies of the vortex, result in greater resistance of the vortex to vertical tilting by an imposed vertical shear flow.

To determine where in the alignment phase space the quasi mode is relevant to the vortex dynamics, we have examined the solution in each case for evidence of a quasi mode. The presence of a quasi mode causes the PV asymmetry associated with the vortex tilt to exhibit a discretelike structure, propagating around the mean vortex with little change in radial structure in time (RM01; SMR; Schecter and Montgomery 2003). For the finite Rossby number Gaussian vortex, Schecter and Montgomery (2003) proved that the quasi mode must decay in time and that the rate of decay is exponential, as anticipated by the QG theory of SMR. Cases in which the tilt evolution displays an exponential decay with time are denoted by ''Q'' in Fig. 3. Consistent with the QG results of Fig. 2, the quasi mode is present for the chosen range of $L/l_{r,G}$ at small Rossby number. When $L/l_{r,G}$ is small compared to unity, the quasi mode persists for Ro $\gg 1$.

As $L/l_{r,G}$ increases, a demarcation in solution with increasing Rossby number becomes evident. The vortex ceases to reflect the presence of a quasi mode. Since the perturbation radial velocity vanishes in this limit of small local Rossby deformation radius (see RM01 for details), the radial advection of mean PV in the linearized PV equation [see Eq. (13)] can be neglected compared to the azimuthal advection term (i.e., the advection of perturbation PV by the *mean* tangential wind). In this limit perturbation PV is then passively advected around the vortex. RM01 referred to this evolution in the QG context as the ''spiral wind-up'' solution (Bassom and Gilbert 1998).

Because the PE perturbation PV evolution is largely balanced, we employ the expression for AB pseudo-PV,

$$\frac{N^2}{r}\frac{\partial}{\partial r}\left(\frac{r}{\overline{\xi}}\frac{\partial\hat{\phi}_{11}}{\partial r}\right) - \frac{N^2}{\overline{\xi}}\left[\frac{(2\overline{\xi}-\overline{\eta})}{\overline{\eta}r^2} + \frac{1}{l_r^2(r)}\right]\hat{\phi}_{11} = \hat{q}_{11}, \quad (17)$$

to diagnose the finite Rossby number tilt evolution $|\hat{\phi}_{11}|$ in the spiral wind-up limit, and then compare it to the linear PE simulated result. For *pure* spiral wind-up behavior the pseudo-PV perturbation evolves as

$$\hat{q}_{11}(r, t) = \hat{q}_{11}(r, 0)e^{-i\overline{\Omega}(r)t}, \quad (18)$$

where $\hat{q}_{11}(r, 0)$ is the initial pseudo-PV amplitude. The geopotential amplitude $|\hat{\phi}_{11}|$ is then obtained by inverting Eq. (17) at each time. In the region of the phase space denoted by ''S'' in Fig. 3 the tilt asymmetry evolution is approximated well by the AB spiral wind-up solution (18) out to at least $t = 10\tau_e$. On this basis we conclude that Gaussian vortices in this regime do not support *long-lived* quasi modes. The physical mechanism for alignment in this region of the phase space is the redistribution of PV by sheared VRWs. To illustrate the vortex evolution in the quasi mode and spiral wind-up regimes we show results from two representative simulations.

2) Alignment by spiral wind-up

In the first experiment we examine the self alignment of a vortex with $L = 100$ km, $V_{\max} = 40$ m s^{-1}, and $l_{r,G} = 154$ km. According to Fig. 2, QG theory at $L/l_{r,G} = 0.65$ would predict precession of the vortex with little decay of the tilt over several τ_e. The actual evolution of the vortex shown in Fig. 4 with Ro $= 3.9$ is dramatically different. In Fig. 4a we see that the asymmetric PV at $z = 0$ undergoes a spiral wind-up similar to the small $l_{r,G}$ results of RM01 (see their Fig. 10). It should be made clear, however, that the evolution of asymmetric PV is not explained simply by passive advection. Radius–time plots of the PV amplitude (not shown) indicate the outward propagation and stagnation of wave packets. Since gravity waves have minimal reflection in the PV core and the internal gravity wave speed $c_m = 16$ m s^{-1} is much greater than the approximately 4 m s^{-1} observed radial group velocity, the outward propagating features must be VRWs. One might reasonably conclude then that the mechanism for the alignment of the vortex in this part of the phase space is the same VRW process identified by RM01 in the QG context at large $L/l_{r,G}$.

Figure 4b further supports this VRW interpretation. Shown is the vortex tilt as a function of time out to $t = 10\tau_e$. Consistent with the findings of Montgomery and Kallenbach (1997, and references therein), as the perturbation PV disperses on the mean vortex as sheared VRWs, the perturbation geopotential decreases in amplitude. This decrease occurs rapidly, with the geopotential approaching approximately 20% of its initial value in less than $2\tau_e$. The balanced nature of this rapid alignment process is evidenced by the good agreement between PE and AB simulations. A pure spiral wind-up solution derived from Eqs. (17)–(18) is also plotted in Fig. 4b. As already indicated in Fig. 3, the simulated decay of vortex tilt follows the spiral wind-up solution. The oscillations in amplitude, which are present in both the PE and AB models, result from the radial propa-

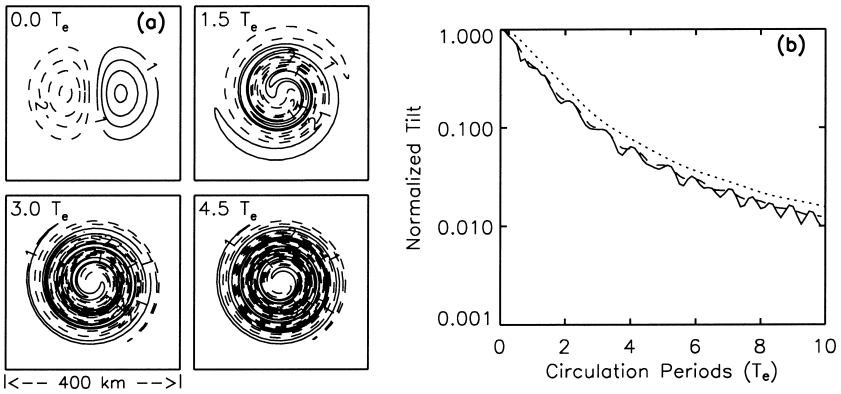

FIG. 4. Gaussian vortex alignment at Ro = 3.9 in a regime where QG theory predicts precession ($L/l_{r,G} = 0.64$). (a) Evolution of the azimuthal wavenumber-1 component of Boussinesq PV at $z = 0$ (contour interval 1×10^{-8} s^{-3}) showing axisymmetrization in the vortex core; and (b) log-linear plot of vortex tilt (normalized by the initial value) over a $10\tau_e$ period from the linear PE model (solid), linear AB model (dashed), and spiral wind-up solution (dotted). See text for details on the spiral wind-up solution.

gation of VRWs past the radius of maximum mean PV gradient used to compute the vortex tilt.

3) ALIGNMENT BY QUASI-MODE DECAY

In the second experiment the same mean vortex is used, but with Ro = 6.5. More significantly $l_{r,G} = 630$ km, yielding $L/l_{r,G} = 0.16$. The PV evolution shown in Fig. 5a strongly suggests the presence of an underlying discrete VRW structure. Although wavelets are observed to propagate radially outward, as in the previous case, the PV asymmetry as a whole shows a distinct cyclonic azimuthal propagation with a distinct azimuthal phase speed of approximately one-fifth $V_{\max}$. The radius at which the phase speed equals the rotation speed of the vortex, the critical radius, falls at $r = 250$ km. This location is outside the vortex core in a region of near-zero mean radial PV gradient. According to the finite Rossby number vortex alignment theory of Schecter and Montgomery (2003), the exponential decay rate of the quasi mode is proportional to the radial gradient of mean PV at the critical radius. Figure 5b confirms the presence of the quasi mode because the tilt asymmetry at long times decays slowly at an exponential rate.[2]

Although the quasi mode ultimately dominates the solution, over the first τ_e the vortex tilt decays more like the spiral wind-up evolution of the previous experiment. This ''adjustment'' of the vortex at early times is found to be characteristic of all simulations in the quasi mode regime of the alignment phase space. The adjustment becomes more pronounced as the Rossby number is increased. It is not an adjustment accomplished by gravity wave radiation since the PE and AB

[2] The quantitative discrepancy between the PE and AB decay rates is a consequence of the large (>1) values of the AB expansion parameter, $\mathcal{D}_I^2 \equiv (\partial/\partial t + \overline{\Omega}\partial/\partial\lambda)^2/\overline{\eta}\overline{\xi}$, outside the vortex core for a Gaussian vortex supporting a quasi mode. See Schecter and Montgomery (2003) for further discussion.

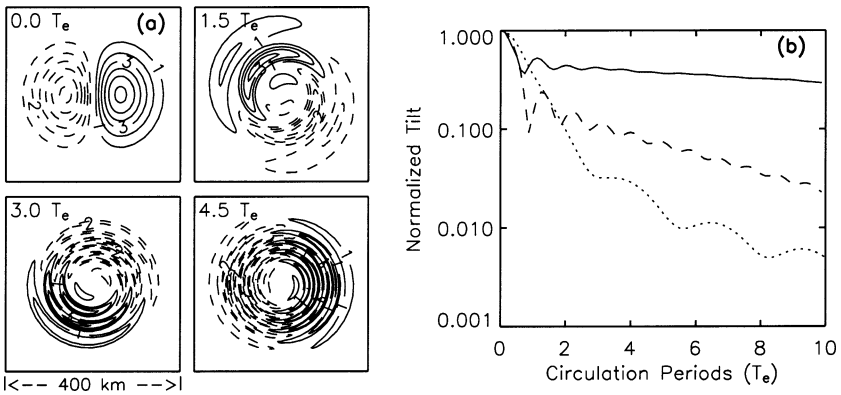

FIG. 5. As in Fig. 4 but for Ro = 6.5 and $L/l_{r,G} = 0.16$. The initial rapid decay of vortex tilt over the first τ_e is a consequence of the tilt asymmetry projecting strongly onto sheared VRWs. At later times the tilt decays exponentially, consistent with a resonantly damped VRW.

models agree in its timing. The adjustment results from the ''mismatch'' between the simple tilt initial condition [Eq. (16)] and the quasi mode radial structure. In the QG theory, the two were approximately identical (RM01; SMR). Schecter and Montgomery (2003) have shown that at finite Rossby number the quasi mode no longer takes the form of a simple, spatially uniform tilt. The general initial tilt perturbation then evolves toward the quasi-mode structure through the radiation of sheared VRWs, in a manner similar to that described by RM01 for general perturbations in the QG context. Thus, at large Rossby number and for simple tilts, while the quasi-mode decay accounts for the latter portion of the overall tilt decay on the time scales presented, the bulk of the alignment takes place rapidly at early times through the axisymmetrization of PV via the sheared VRW mechanism.

4. A heuristic model for a distributed vortex in vertical shear

From the linear VRW perspective there are three ways in which the vortex in shear remains vertically aligned. In the absence of a quasi mode, the tilt perturbation generated by differential advection of the vortex by the shear flow will disperse on the mean vortex as sheared VRWs. If the axisymmetrization of the perturbation PV (i.e., the tilt) can counter the production by differential advection, then the vortex will remain upright. When a vortex supports a quasi mode, we found in the previous section that the tilt evolution in the unforced case is actually a superposition of the sheared VRWs and the quasi mode. In this case the resulting evolution should reflect both parts of the solution, but may be dominated by the latter if it is more robust. In the free alignment example of Fig. 5 the quasi mode was observed to decay at a much slower rate than the transient sheared VRWs. It stands to reason, then, that the forced solution will tend to ''lock on'' to the less evanescent quasi-modal part. If the quasi mode dominates the evolution, then the vortex resists tilting by vertical shear in two ways, through precession upshear (similar to the mechanism described by SJ95) and resonant damping. Regardless of whether or not a quasi mode exists, the mechanism for vortex tilt reduction is VRW damping.

In that part of the free-alignment phase space where *decaying* quasi modes exist, Schecter and Montgomery (2003) found the vortex tilt PV takes the form of a damped discrete VRW (for $n = 1$):

$$q'(r, \lambda, z, t) = \mathrm{Re}[C(r, z)e^{\gamma t}e^{i(\lambda-\omega_p t)}], \qquad \gamma < 0, \quad (19)$$

where $C(r, z)$ provides the radial and vertical structure of the tilt, γ is the exponential damping rate, and ω_p is the vortex precession frequency. In the derivation of Eq. (19) it is assumed that $|\gamma/\omega_p| \ll 1$. The temporal part of Eq. (19) is the solution to a differential equation of the form

$$\frac{dq'}{dt} + (i\omega_p - \gamma)q' = 0. \quad (20)$$

This equation can be motivated physically from a recasting of the linearized PE PV equation or, since the perturbation evolution is largely balanced, the AB pseudo-PV equation. Consistent with the balanced VRW dynamics, Eq. (20) describes a single-component damped harmonic oscillator.

If we now view the vertical shear as a time-invariant forcing [cf. Eq. (12)], Eq. (20) can be generalized to that of a forced damped harmonic oscillator. For zonal vertical shear flow the associated PV has a horizontal gradient in the y direction, and the forcing on the rhs is of the form $2F_{q,s}(r, z)\cos\lambda$. The solution to the forced equation is

$$q'(r, \lambda, z, t) = \mathrm{Re}\left[A(r, z)e^{\gamma t}e^{i(\lambda-\omega_p t)} + \frac{2F_{q,s}}{i\omega_p - \gamma}\frac{e^{i\lambda}}{2}\right], \quad (21)$$

where $A(r, z)$ is a complex amplitude. Assuming the initial vortex is vertically aligned, that is, $q'(t = 0) = 0$, and utilizing the fact that $|\gamma/\omega_p| \ll 1$, it follows from (21) that

$$q'(r, \lambda, z, t) \approx -\frac{F_{q,s}(r, z)}{\omega_p}[e^{\gamma t}\sin(\lambda - \omega_p t) - \sin\lambda]. \quad (22)$$

Therefore, for small but finite $|\gamma/\omega_p|$ the long-time solution will always be one of fixed tilt, oriented perpendicular to the direction of shear, or downshear-left. The *downshear-left configuration* is *optimal* because the vertically penetrating flow associated with the tilted PV of the vortex has a *vertical shear opposite in sign* to the environmental vertical shear flow (SJ95). For stable vortex profiles (i.e., $\gamma \leq 0$), the counteracting vertical shears across the vortex core make the equilibrium solution a possibility. Figure 6a illustrates schematically the vortex tilt evolution in this case. It should be noted, however, that the basis for assuming solutions of the form given by Eq. (19) becomes more tenuous as $|\gamma/\omega_p|$ approaches unity. In this regime SMR demonstrated that the quasi mode rapidly disperses on the mean vortex as sheared VRWs, and thus this simple harmonic oscillator analogy no longer holds.

Recall from section 3 that in the TC regime ($L/l_{r,G} \sim 0.1$) the tilt of a Gaussian vortex supporting a quasi mode decays at a very slow rate on the time scale of the vortex precession. In this case $\gamma \approx 0$, and we arrive at the solution for a forced undamped harmonic oscillator:

$$q'(r, \lambda, z, t) = -\frac{F_{q,s}(r, z)}{\omega_p}[\sin(\lambda - \omega_p t) - \sin\lambda]. \quad (23)$$

For all values of ω_p this solution represents the perpetual tilting, precession, and realignment of a vortex in zonal

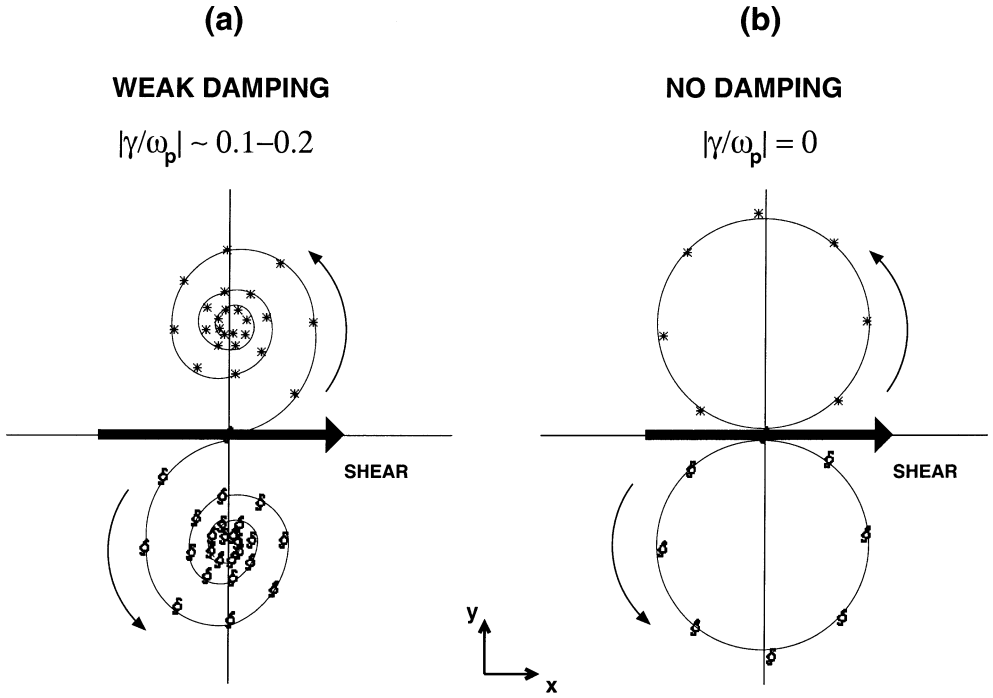

FIG. 6. Schematic illustration of the vortex tilt evolution [based on Eq. (22)] for the case where (a) the VRW damping rate γ is a nonnegligible fraction of the precession frequency ω_p and (b) the VRW damping rate is zero. The initially aligned vortex is tilted by westerly vertical shear. The vortex center at upper levels is denoted by the stars and at lower levels by the hurricane symbols. The thin arrows indicate the direction of motion of the upper- and lower-level centers. The vortex in (a) achieves a steady-state tilt to the left of the vertical shear vector. In (b) the vortex tilts downshear, precesses cyclonically upshear, realigns, and then repeats this evolution.

shear. Figure 6b depicts the vortex tilt evolution in the limit of infinitesimal damping.

This linear harmonic oscillator model of the vortex in shear breaks down once the vertical tilt becomes sufficiently large. Smith et al. (2000) showed that, as the vertical shear is increased, an idealized vortex can be made to transition from a regime where the vortex precesses to one where the upper- and lower-level PV anomalies of the vortex separate indefinitely [the Smith et al. model does not, however, permit initially aligned vortices to achieve steady-state solutions of the form given by Eq. (22)]. The irreversible separation of upper- and lower-level PV anomalies is fundamentally nonlinear, and occurs when the vortex is unable to precess quickly enough to overcome the differential advection by the shear flow. In the upcoming discussion we characterize the ''breaking point'' of the vortex in shear by the time it takes the horizontal distance between upper- and lower-level PV centers to increase by twice the RMW, $2L$, under simple advection by the shear flow. For the shear flow defined by Eq. (9) the differential advection rate $\tau_s^{-1} \sim U/L$.

5. Vortex alignment in vertical shear: Numerical simulations

To further understand how the VRW damping mechanism described in the previous sections keeps the vortex vertically aligned when a vertical shear flow is imposed, we continue our investigation using the simple linearized PE model forced by a time-invariant zonal vertical shear flow. As described in section 2, the shear flow is chosen such that it projects only onto the first internal vertical mode, and thus forces a vertical tilt similar to that given by Eqs. (15)–(16). Any complete study of TC-like vortices in vertical shear must ultimately permit the shearing apart of the vortex as a possible solution, which the linear model obviously does not allow. But in the parameter regime for which the linear approximation is reasonably accurate (i.e., overlapping upper- and lower-level PV cores), it serves as a useful first approximation for understanding the basic dynamics. For the idealized vortex simulations presented below all linear results are compared against simulations using the fully nonlinear dry dynamical core of the CSU–RAMS model.

a. Vortex resiliency in shear

Consider a weak vortex ($V_{\max} = 10$ m s^{-1}, $L = 100$ km) with Ro $= 3.2$ and $L/l_{r,G} = 0.08$ in easterly vertical shear of 4 m s^{-1} ($U = 2$ m s^{-1}) over a 10-km depth. According to Fig. 3, the vortex exhibits little tendency for alignment as it is dominated by a weakly decaying quasi mode. In this case the precession frequency $\omega_p = 5.26 \times 10^{-6}$ s^{-1} is an order of magnitude less than the

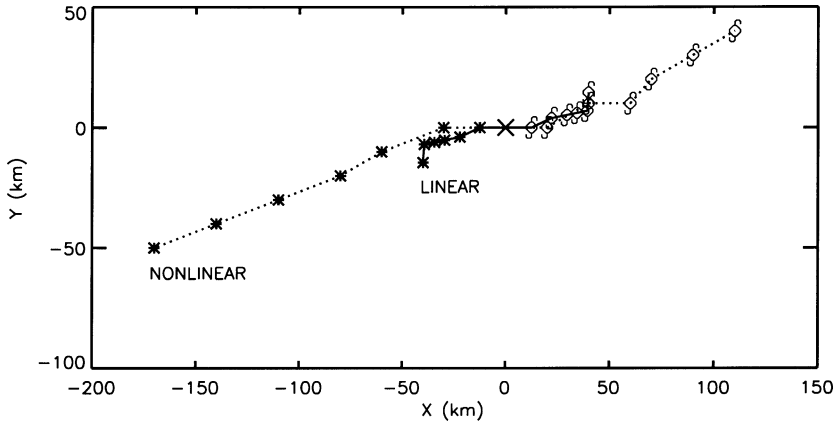

FIG. 7. Evolution of an initially upright Gaussian vortex in easterly vertical shear of 4 m s^{-1} (10 km)$^{-1}$. Shown are the locations of the PV maxima every $\tau_e/4$ at $z = 0$ (hurricane symbols) and $z = 10$ km (stars). The vortex is of tropical depression strength ($V_{max} = 10$ m s^{-1}) with Ro = 3.2 and $L/l_{r,G} = 0.08$, placing it well within the quasi-mode regime of Fig. 3. The initial shearing apart of the vortex is well captured by the linear PE model (solid). A long-time shearing apart of the vortex is predicted by the nonlinear RAMS model (dotted).

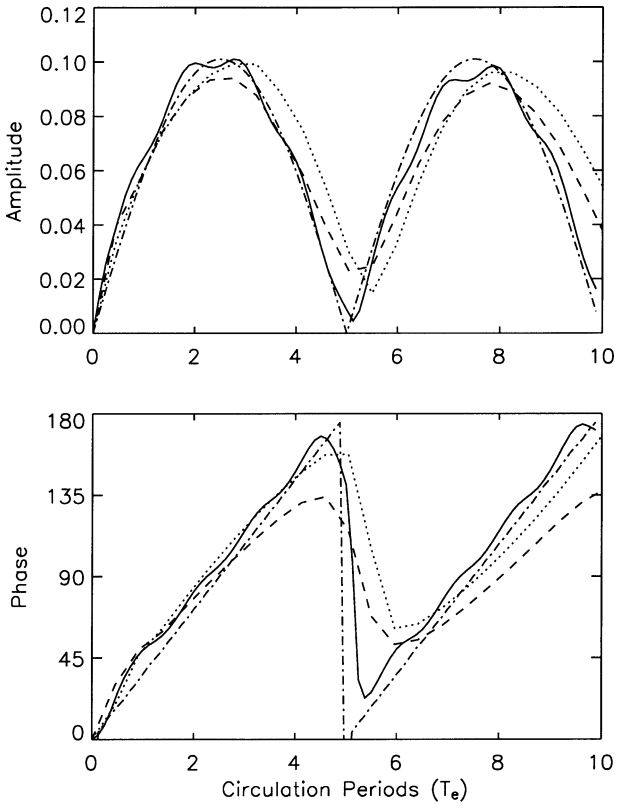

FIG. 8. Amplitude (normalized by the maximum mean PV) and phase of the azimuthal wavenumber-1 PV asymmetry for the hurricane-strength (40 m s^{-1}) Gaussian vortex. All parameters are as in Fig. 7, except Ro = 12.7. The vortex remains vertically coherent by precessing upshear (180°) and realigning. The linear evolution (solid) agrees well with the nonlinear RAMS simulation at $z = 0$ (dashed) and $z = 10$ km (dotted), and also with the forced undamped harmonic oscillator solution based on Eq. (23) (dashed–dotted). For simplicity we have normalized the harmonic oscillator solution to match the maximum amplitude of the linear PE solution.

differential advection rate $\tau_s^{-1} = 2 \times 10^{-5}$ s^{-1}. The evolution of the upper- and lower-level PV maxima shown in Fig. 7 reflects the relatively slow precession of the quasi mode. Little meridional displacement compared to zonal displacement is observed. In the RAMS simulation the zonal displacement, while in agreement with the basic trend shown in the linear simulation at early times, is much more dramatic, with the vortex completely shearing apart after $t = 1\tau_e$. The linear solution is still useful because it suggests that, when γ and ω_p are much less than τ_s^{-1}, the vortex will tend to shear apart.

Keeping all else the same, but increasing Ro to 12.7 ($V_{max} = 40$ m s^{-1}, $L = 100$ km), a very different vortex evolution is observed. Figure 8 shows time series of the azimuthal wavenumber-1 PV amplitude (normalized by the maximum mean PV of the vortex) and phase associated with the tilt asymmetry. As in the small Rossby number case, the vortex first tilts in the direction of the vertical shear. The PV perturbation in this case, however, never reaches a significant fraction of the mean PV. Thus, the vortex remains nearly aligned at all times, and the nonlinear RAMS solution is well approximated by the linear solution. The vortex precesses upshear, realigns, and then repeats the process over again. Such an evolution was anticipated in the previous section when γ is negligible and $\omega_p > \tau_s^{-1}$. Here $\omega_p = 8 \times 10^{-5}$ s^{-1}, which is larger than $\tau_s^{-1} = 2 \times 10^{-5}$ s^{-1}. The tilt decay at long times is approximately zero, so the conditions for the forced undamped harmonic oscillator are satisfied. The forced undamped solution (23) is plotted in Fig. 8. It agrees well with the linear PE solution, as expected.

Suppose we now increase the vertical shear in this large Rossby number case. How strong must the shear get before the vortex shears apart, and what determines

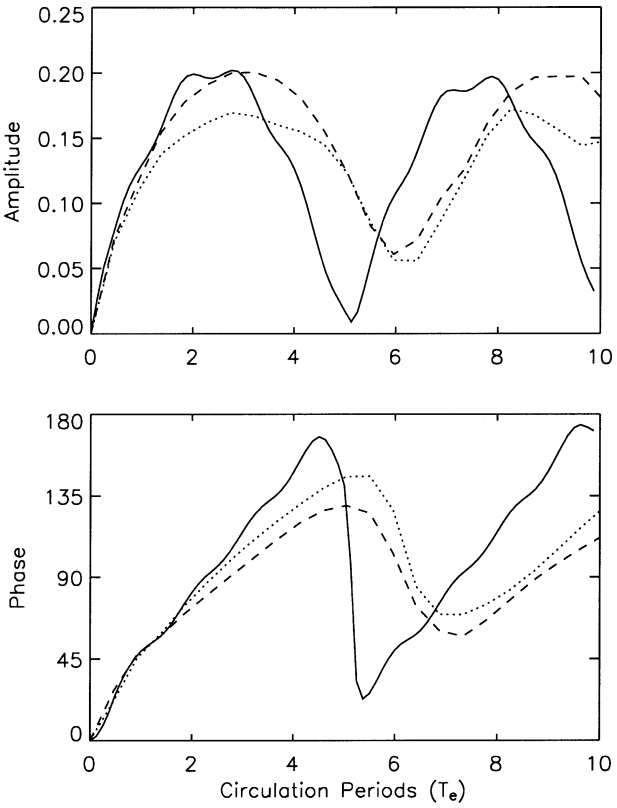

FIG. 9. As in Fig. 8 but with stronger easterly vertical shear of 8 m s^{-1} (10 km)$^{-1}$.

that threshold? Is it simply a matter of the quasi mode not being able to precess quickly enough? Using the RAMS model, we illustrate in Fig. 9 the changes in vortex behavior with increasing vertical shear. At 8 m s^{-1} over a 10-km depth, the upper- and lower-level vortex PV remains vertically aligned in the RAMS simulation, precessing as in the weaker shear case but at a slightly slower cyclonic speed. The linear precession frequency ($=8 \times 10^{-5}$ s^{-1}) is still found to be twice the differential advection rate ($=4 \times 10^{-5}$ s^{-1}), so the continued resiliency of the vortex is not surprising based on our simple arguments. The actual tilt of the vortex PV is shown in Fig. 10. When the vortex reaches its maximum tilt at 90°, the horizontal separation between upper- and lower-level PV maxima reaches approximately 60 km (Fig. 10a). As also noted by SJ95, the tilt of the inner core of the vortex is noticeably less than that of the larger-scale vortex. Since the vortex evolution is largely balanced, one need not invoke the divergent part of the circulation to explain this structure—the transverse circulation exists to maintain balance (RM01). Consistent with our VRW theory for vortex alignment, the radial vortex structure is, instead, a consequence of the emergence of the quasi mode. As previously discussed [see section 3c(3)], the quasi mode at finite Rossby number does not take the form of a simple, spatially uniform tilt perturbation (as it does in the QG theory). Thus, the superposition of the mean vortex and the emerging quasi mode will yield a vortex tilt that is spatially nonuniform, as shown in Fig. 10. As the vortex continues to precess upshear, both the vortex core and large-scale vortex realign (Fig. 10b).

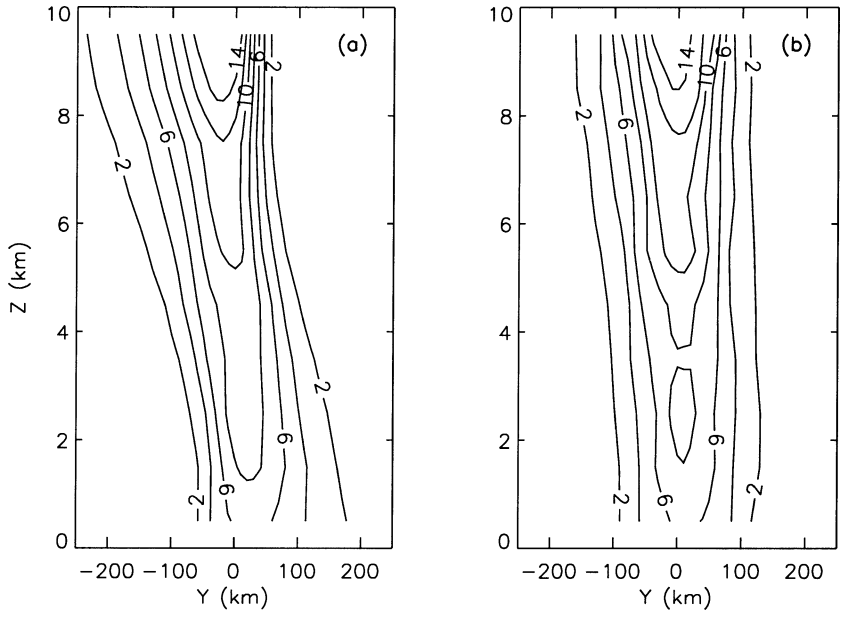

FIG. 10. Vertical cross section of Ertel PV in the direction of tilt (90°) at (a) $t = 3\tau_e$ (maximum tilt) and (b) $t = 6\tau_e$ (realignment) for the nonlinear RAMS simulation of Fig. 9. Values are in PVU, where 1 PVU $= 10^{-6}$ m^2 s^{-1} K kg^{-1}. Notice the tilt of the vortex core is smaller than that of the larger-scale vortex.

When the vertical shear equals 12 m s^{-1} (10 km)$^{-1}$ the vortex appears to begin to shear apart at early times, but subsequently realigns and stays vertically coherent (not shown). A new phenomenon arises at this larger value of shear not seen at 8 m s^{-1} (10 km)$^{-1}$. As the vortex tilt becomes large and the local vertical shear of the vortex winds also increases, the gradient Richardson number, defined as $N^2/[(\partial u/\partial z)^2 + (\partial v/\partial z)^2]$, drops below unity in localized regions of the vortex core. A local instability occurs within these regions, verified with horizontal grid spacing of $\Delta x = \Delta y = 10$ km and $\Delta x = \Delta y = 2$ km. In both cases the vertical grid spacing $\Delta z = 1$ km. The PV in these localized regions becomes large, implicating an upgradient transfer due to subgrid-scale processes [cf. Thorpe and Rotunno (1989) section 2]. We speculate that the mixing that accompanies this instability is not well resolved at the present RAMS vertical resolution. The instability ultimately ceases, though, and the vortex relaxes to a smooth, vertically coherent structure. Further investigation of this behavior for strong vortices in strong shear will be reported upon in a forthcoming publication.

b. Comparison with previous work

The results presented here using the vortex given by Eq. (14) differ from those of SJ95. The large Rossby number simulation depicted in Fig. 8 uses vortex and environmental parameters very similar to those used by SJ95 in her benchmark simulation. When embedded in 4 m s^{-1} (10 km)$^{-1}$ vertical shear, the tilt of her vortex increased steadily throughout the duration of the 96-h simulation. Our vortex remains vertically coherent with only a small departure from an aligned state at any time. The primary difference between the two simulations is the radial structure of the initial vortex. The vortex profile used by SJ95 is shown in Fig. 11. Although her vorticity profile closely resembles our monotonically decreasing Gaussian within the RMW, outside the approximately 170-km radius the relative vorticity becomes negative and then asymptotes to zero at large radius. Similar barotropic profiles used by Gent and McWilliams (1986) were found to support an internal instability in the QG system, which could be interpreted in our problem as a ''tilt instability.''

To test whether the susceptibility of the SJ95 benchmark vortex to vertical shear could simply be a consequence of this tilt instability generalized to finite Rossby number, we perform a free alignment simulation using the linear PE model as in section 3, but with the SJ95 profile. The results are shown in Fig. 12a. A transient decay of the vortex tilt is quickly followed by exponential growth through the duration of the simulation with a growth rate of 2.2×10^{-5} s^{-1}. Thus, even without vertical shear the vortex is prone to shearing apart. When the 4 m s^{-1} (10 km)$^{-1}$ vertical shear is added in the linear PE model, the results are quite similar to the nonlinear PE benchmark simulation results of

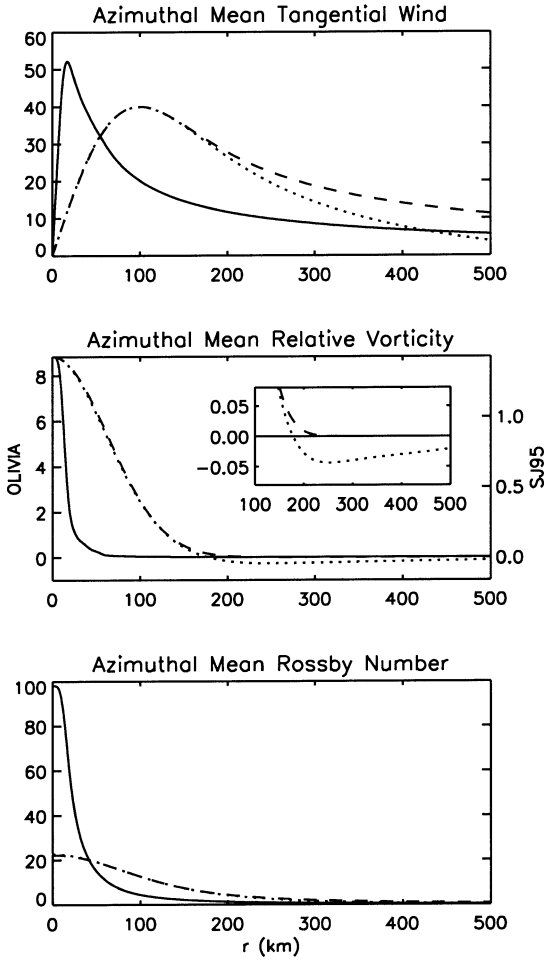

FIG. 11. The azimuthal-mean vortex used in the Hurricane Olivia (solid) and SJ95 (dotted) simulations. Also shown is the 40 m s^{-1} Gaussian vortex used in Fig. 8 (dashed). The tangential wind and relative vorticity are in units of m s^{-1} and 10^{-3} s^{-1}, respectively. The relative vorticity inset shows the radial structure of the SJ95 vortex outside the RMW. The Rossby number, Ro $= \overline{v}(r)/fr$, is based on the azimuthal mean tangential velocity of the untilted vortex.

SJ95 out to approximately $t = 3\tau_e$, as shown in Fig. 12b (compare with the SJ95 Fig. 2).

It is tempting to speculate on the cause of the exponential tilt growth in the SJ95 free alignment simulation based on the recent extension of resonant damping theory to finite Rossby number by Schecter and Montgomery (2003). According to the resonant damping theory [i.e., Eq. (19)], the growth/decay rate γ of the tilt perturbation is proportional to the mean PV gradient at the critical radius in the flow where the precession frequency equals the vortex rotation. For the Gaussian vortex γ is always negative, and damping occurs. But for the SJ95 vortex it is possible for γ to be positive, and hence for resonant *growth* to occur. Upon calculating the precession frequency of the growing tilt perturbation in the SJ95 simulation ($\omega_p = 4.7 \times 10^{-5}$ s^{-1}), we find that the location in the flow where resonance would

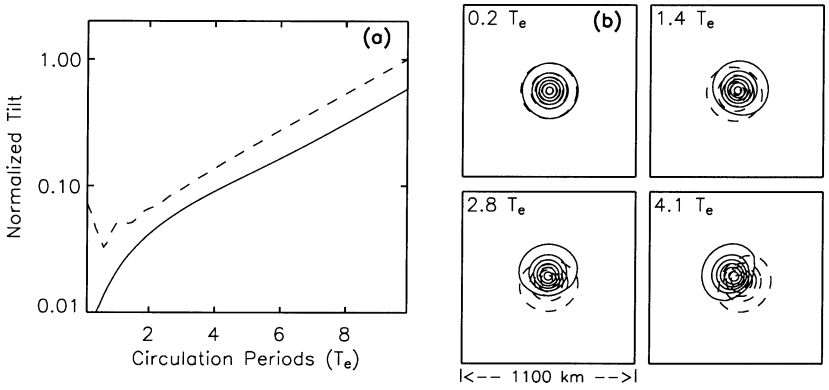

FIG. 12. Linear PE evolution of the benchmark vortex described in SJ95 subjected to easterly vertical shear of 4 m s^{-1} (10 km)$^{-1}$. (a) Loglinear plot of vortex tilt from the unforced (dashed) and forced (solid) simulations (normalized by the maximum unforced value). The initial tilt amplitude in the unforced simulation is $\alpha = 0.3$. The vortex is unstable to small tilt perturbations. (b) Total Boussinesq vortex PV at $z = 0$ (solid) and $z = 10$ km (dashed) (contour interval 0.4×10^{-7} s^{-3}).

occur falls within the region of *positive* PV gradient at approximately 300-km radius (see Fig. 11; recall $d\overline{q}/dr = N^2 d\overline{\zeta}/dr$). Further examination of the possible link between the tilt instability of Gent and McWilliams (1986) and resonant growth is reserved for a future publication.

In Jones (2000a) the benchmark vortex profile of SJ95 was used in a simulation similar to that described above, but at higher latitude. The vertical tilt initially increased as the vortex precessed upshear, but then decreased as the vortex achieved a downshear orientation. Jones (2000a) showed that this behavior results from advection of the vortex core by large-scale asymmetries generated by the vertically penetrating flow of the tilted vortex. These large-scale asymmetries only have significant impact as the vortex tilt becomes large and when they are allowed to remain as robust features outside the vortex core. By broadening the vortex profile (and thus moving the region of negative relative vorticity farther from the vortex core), Jones (2000a) showed that the vortex remains vertically coherent at long times, behaving as our sheared hurricane-strength Gaussian vortex. We have verified using our linear model that the critical radius for the vortex in this case (see her Fig. 13, case NP2) falls in a region of small but negative mean vorticity gradient, and thus does not support a tilt instability.

c. *Hurricane Olivia (1994)*

As our final example, we apply the VRW damping ideas developed in the foregoing to the case of Hurricane

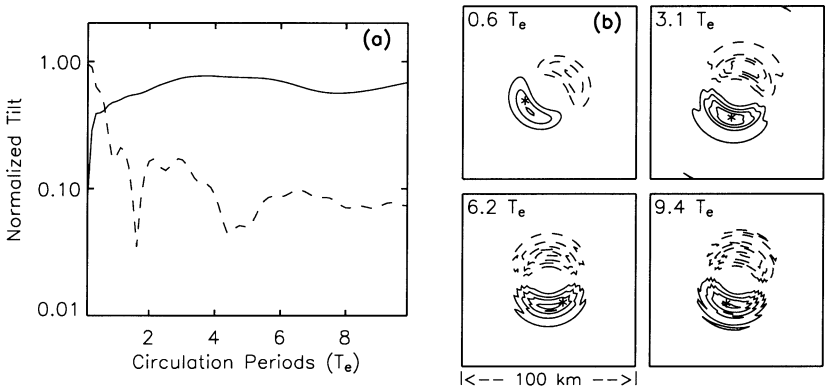

FIG. 13. Linear PE evolution of the Olivia vortex (Ro $\sim$ 68 and $L/l_{rG} \sim 0.02$) subjected to westerly vertical shear of 10 m s^{-1} (10 km)$^{-1}$. (a) Vortex tilt from the unforced (dashed) and forced (solid) simulations (normalized by the maximum unforced value). The initial tilt amplitude in the unforced simulation is $\alpha = 0.3$. (b) Azimuthal wavenumber-1 component of Boussinesq PV at $z = 0$ (contour interval 0.5×10^{-7} s^{-3}). Stars denote the phase evolution predicted by the forced damped harmonic oscillator solution (see text for details). The long-term solution is a steady-state tilt (south to north with height) to the left of the westerly shear vector.

Olivia (1994). The vortex profile shown in Fig. 11 is taken from the observational study of Olivia by Reasor et al. (2000). Olivia was observed to weaken from ''top down'' as north-northwesterly vertical shear increased from 2–3 m s^{-1} to 15 m s^{-1} over the lowest 10-km depth of the storm in a 4-h period. The vortex tilt in the lower to middle troposphere was approximately 2–3 km with a west-to-east orientation with height. Olivia's wind structure before encountering the large vertical shear consisted of a prominent barotropic component. For simplicity, we assume the mean vortex is initially barotropic. We have also artificially filled the eye with cyclonic vorticity in order to eliminate the emergence of barotropically unstable modes, discussed by Reasor et al. (2000). Using $H = 10$ km, $f = 4.5 \times 10^{-5}$ s^{-1}, $N = 1.22 \times 10^{-2}$ s^{-1}, $L = 17$ km, and $V_{\max} = 52$ m s^{-1} yields Ro = 68 [note that here Ro = $V_{\max}/fL$, whereas Schecter and Montgomery (2003) define Ro = $\zeta(0)/f$] and $L/l_{r,G} = 0.02$. Although Fig. 3 is strictly valid for Gaussian-like vorticity profiles, it suggests that, if the results were extrapolated to very large Rossby number, the Olivia vortex might support a quasi mode. In Fig. 13a we show the free alignment of the Olivia vortex. It is difficult to discern the presence of a quasi mode given the high amplitude oscillations in vortex tilt. Schecter and Montgomery (2003) have indeed verified the presence of a rapidly decaying quasi mode for the Olivia case (see their Fig. 11). Due to its rapid decay with time, however, it is unclear whether it will dominate the forced solution in the way the quasi mode apparently dominated the evolution of the large Rossby number Gaussian vortex in vertical shear.

When westerly vertical shear of 10 m s^{-1} (10 km)$^{-1}$ is imposed, Fig. 13a shows that the vortex tilt remains small for the duration of the simulation, never quite reaching the initial small tilt of the free alignment experiment. In this case $\tau_s^{-1} = 2.94 \times 10^{-4}$ s^{-1}, less than the precession frequency $\omega_p = 3.9 \times 10^{-4}$ s^{-1} determined by Schecter and Montgomery (2003). Thus, we would expect the linear results to be at least qualitatively accurate. According to Fig. 13b, the vortex tilts from west to east with height at early times, consistent with the direction of the vertical shear. The vortex precesses cyclonically, as in previous simulations but only rotates through 90°, reaching a near-steady-state tilt configuration downshear-left of the vertical shear.[3] This type of evolution was predicted in section 4 for the case of nonnegligible quasi-mode decay rate. Inserting the values of γ (-4.86×10^{-5} s^{-1}) and ω_p (3.9×10^{-4} s^{-1}) determined by Schecter and Montgomery (2003) into the forced damped harmonic oscillator Eq. (22), the PV phase evolution is approximately reproduced, as indicated in Fig. 13b.

6. Summary and discussion

We have presented a new theory for the resiliency of initially barotropic and stable TC-like vortices in vertical shear flow, demonstrating the fundamental role of VRWs in the maintenance of vortex vertical alignment and the remarkable ability of such vortices to withstand strong vertical shear (>10 m s^{-1} over the depth of the troposphere) without the direct aid of cumulus convection. Previous studies have invoked the concept of penetration depth to account for the ability of dry TC-like vortices to fight differential advection by vertical shear, and thus remain vertically coherent. While this view is both physical and conceptually appealing, it is incomplete. It cannot explain, for example, the subtle dependence of the TC evolution on radial profile as demonstrated here, the presence of quasi-stationary tilted states for the TC in shear (e.g., downshear-left), and the prominence of radially and azimuthally propagating VRWs that arise when a strong TC is forced by vertical shear. The theory presented here sheds light on all of these issues, exposing clearly the quasi-elastic nature of a stable TC and the VRWs that are intrinsic to such a vortex.

Vertical shear acts as a VRW generator when it interacts with a TC. To illustrate this we began by considering the free alignment of finite Rossby number vortices. Given a simple vertical tilt, a vortex with monotonically decreasing mean PV will align through the projection of the tilt asymmetry onto stable VRWs. Vortices for which $L/L_{r,G} \ll 1$ are likely to support a near-discrete VRW, or quasi mode, especially at small Rossby number. The quasi-mode propagation causes the vortex to precess, and its decay leads to slow alignment. Schecter and Montgomery (2003) have developed a theoretical formalism for studying the quasi mode at finite Rossby number by which the linear damping rate and precession frequency can be determined. We have demonstrated, however, that not all vortices support quasi modes within the parameter regime typical of TCs. Specifically, a vortex for which the horizontal scale is a nonnegligible fraction of the global internal deformation radius and Ro $\gg 1$ will instead align through the dispersion of the vortex tilt asymmetry on the mean vortex as sheared VRWs. The inviscid damping of the sheared VRWs then leads to rapid reduction of the vortex tilt.

When vertical shear is applied to an initially aligned vortex, the TC not supporting a quasi mode will counter the production of vertical tilt by differential advection through sheared VRW dispersion. On the other hand, the evolution of a TC-like vortex supporting a quasi mode was shown to be dominated by the quasi mode when it is forced. We know from Schecter and Montgomery (2003) that the free-alignment solution is simply that of a damped harmonic oscillator in the limit of small

[3] The linear PE results have been verified using the nonlinear RAMS model. Although RAMS is non-Boussinesq, and thus the PV is not symmetric about middle levels as in the linear Boussinesq PE model, the vortex still still achieves a steady-state tilt oriented downshear-left.

damping rate γ compared to the precession frequency ω_p. If the shear forcing is time invariant, the resulting forced solution is straightforward.

The precise behavior of the vortex supporting a quasi mode in shear depends on the radial location where ω_p equals the angular rotation rate of the mean flow, what Schecter and Montgomery (2003) define as the ''critical radius.'' The damping rate is proportional to the radial gradient of mean PV at this radius. A Gaussian vortex is characterized by weak PV gradients outside the vortex core, so in the TC regime γ is typically negligible.[4] For meteorologically relevant timescales ($t \leq$ 1–2 days), the Gaussian vortex in shear behaves as a forced undamped harmonic oscillator characterized by the perpetual tilting, cyclonic precession upshear, and realignment of the vortex. Studies of realistic hurricanes in vertical shear typically do not observe such an evolution. The reason for this is that a hurricane profile, unlike the Gaussian, typically exhibits large radial PV gradients at 2–3 times the RMW where the critical radius is likely to fall, leading to more rapid decay of the quasi mode. A heuristic analysis showed that the solution in this case is one of steady-state tilt oriented left of the vertical shear vector. We confirmed this behavior via a linear PE numerical simulation using the observed wind profile of Hurricane Olivia (1994). It should be noted that this evolution is also consistent with that of Wang and Holland (1996, their Fig. 4) who used numerically simulated hurricane profiles. Although they invoked the outflow anticyclone to explain the steady-state tilt configuration, here we show that the cyclonic portion of the vortex alone can explain the downshear-left tilt orientation.

We believe that our demonstration of TC-like vortices achieving approximate steady-state tilts to the left of the shear vector in the dry adiabatic model is significant. While the downshear-left tilt orientation is the one that minimizes the net vertical shear (i.e., the superposition of the vertically penetrating flow of the tilted vortex and the environmental vertical shear flow), and thus would appear to be an optimal configuration, the *possibility* of the *downshear-left solution actually depends* on the details of the *vortex profile*. Previous studies using idealized profiles have given the impression that the precessing solution is a typical one in the small tilt limit. The precession shown by Smith et al. (2000), for example, is a consequence of their point vortex model not permitting decaying quasi-mode solutions. For the SJ95 vortex we have shown that the vortex supports a linear tilting instability, causing growth of the tilt with time, even as the vortex precesses. This early evolution is, in fact, consistent with our forced harmonic oscillator model [Eq. (22)], but with $\gamma > 0$. Although quantitative mesoscale observations of hurricane tilt are limited (Marks et al. 1992; Reasor et al. 2000), and to date few studies have focused on hurricane tilt evolution in full-physics numerical simulations (Wang and Holland 1996; Frank and Ritchie 1999, 2001), the consensus thus far appears to be that hurricanes do not precess continually when forced by vertical shear [although they may wobble due to other mechanisms not discussed here (e.g., Nolan et al. 2001)]. When a hurricane is forced by vertical shear, the observations suggest that the vortex tilt is generally oriented downshear to downshear-left (Marks et al. 1992; Reasor et al. 2000). This orientation is consistent with our dry adiabatic results when the decay rate of the quasi mode is nonnegligible. It then stands to reason that the downshear-left location of convective asymmetry observed in hurricanes forced by vertical shear may be in the first approximation a consequence of the dry adiabatic VRW dynamics.

Having clarified how the tilt of vertically sheared TC-like vortices is reduced, the problem of vortex resiliency was then addressed through comparison of linear PE and dry nonlinear RAMS simulations of TC-like vortices in vertical shear. In the absence of a strong alignment mechanism a TC in vertical shear will be differentially advected by the mean flow, causing the vortex to tilt irreversibly. The linear PE model captures such an evolution until the upper- and lower-level PV cores cease to overlap horizontally. We defined a characteristic time scale for this threshold, $\tau_s \sim 2L/\Delta U$, where $2L$ is twice the RMW and ΔU is the difference in shear flow between upper and lower levels of the vortex. For vortices supporting a quasi mode the RAMS simulation confirmed the shearing apart of the vortex when $\omega_p \ll \tau_s^{-1}$. When $\omega_p > \tau_s^{-1}$, the vortex is able to remain vertically aligned through precession upshear. The linear solution remains valid in this regime. For a 40 m s^{-1} Gaussian vortex with L = 100 km (and $l_{r,G}$ = 1230 km) we found that the vortex remains vertically aligned at shears up to 12 m s^{-1} over 10-km depth. For the Hurricane Olivia (1994) profile the vortex remained vertically coherent in 10 m s^{-1} (10 km)$^{-1}$ vertical shear. Based on these results, we conclude that the dry adiabatic dynamics is capable of maintaining the vertical alignment of strong, approximately barotropic stable vortices in shear greater than 10 m s^{-1} over the depth of the vortex.

To determine precisely what sets the critical threshold between alignment of a TC in shear and the irreversible shearing apart of the vortex, we require a clearer understanding of the role of nonlinear processes in vortex alignment at finite Rossby number (Ro $>$ 1). The comparison of ω_p and τ_s^{-1} is only a crude measure of that threshold. The impact of baroclinic vortex structure on the resiliency of TCs must also be examined since TC

[4] For sufficiently large Ro, vortices with weak vorticity gradients outside their core are in principle susceptible to an exponential Rossby–inertia buoyancy (RIB) instability that involves a resonance between the VRW in the core and an inertia buoyancy wave in the environment. Formally, this can occur when $\mathcal{D}_I^2 = (\partial/\partial t + \overline{\Omega}\partial/\partial\lambda)^2\overline{\eta}\overline{\xi} > 1$ (Schecter and Montgomery 2003). For all of the numerical experiments shown here, we do not observe the RIB instability. The vorticity gradient at the critical radius is evidently sufficiently negative to suppress the RIB instability [see Schecter and Montgomery (2003) for details].

winds are observed to decay up to the tropopause. A recent idealized study of baroclinic vortices in vertical shear by Jones (2000b) illustrates how the weaker vortex circulation at upper levels is especially prone to being stripped away from the rest of the cyclonic circulation below it. How the VRW damping mechanism presented here might shed light on this behavior is currently under investigation.

In light of the present findings, the impact of diabatic processes on TC resiliency needs closer examination. Diabatic processes aid the alignment of TCs *indirectly* through reduction of the static stability in regions of moist ascent and intensification of vortex PV via the low- to midlevel convergence of azimuthal-mean vorticity by the axisymmetric component of the diabatically driven secondary circulation. The former will tend to increase $L/L_{r,G}$, and the latter will increase the characteristic Rossby number and the radial gradient of azimuthal-mean PV. A decrease in the Rossby radius of deformation reduces the intrinsic VRW propagation speed and leads to a greater absolute (ground based) azimuthal propagation speed (Reasor et al. 2000). An increase in Rossby number also will increase the absolute azimuthal VRW propagation speed, or in the present vortex alignment context, the precession frequency of the vortex. We have demonstrated that an increased precession frequency makes the vortex more resilient to differential advection by the vertical shear flow. The increased precession frequency also shifts the critical radius radially inward into a region of larger negative mean PV gradient (which itself may be enhanced by diabatic processes). The increased VRW damping rate makes the vortex even more resilient to vertical shear.

Diabatic processes, however, may not always have a positive impact on vortex alignment. The numerical simulations of Frank and Ritchie (2001) suggest that diabatic processes can have a deleterious impact on mature hurricanes in strong vertical shear through the convective asymmetry generated by the vortex–shear interaction. Subsequent to the development of a pronounced convective asymmetry, they found that a top-down weakening of the hurricane generally ensues. Understanding how diabatic heating modifies the evolution of the quasi mode and the sheared VRWs and why the convective asymmetry of the tilted hurricane can in some cases hinder alignment via the VRW damping mechanism is an important topic worthy of future study.

Note added in proof: Our simulations in section 5e use the tangential wind profile given in Eq. (1) of SJ95, which has since been discovered to contain a typographical error. The impact of this error on the profile is small, and should not affect the basic results of section 5c.

Acknowledgments. This work was supported in part by Office of Naval Research Grant N00014-02-1-0474, National Science Foundation Grant ATM-0101781, and Colorado State University. The first author was supported in part by the National Research Council while a postdoctoral research associate at the Hurricane Research Division of AOML/NOAA. The authors would like to thank Drs Sarah Jones, Mark DeMaria, Yuqing Wang, and Ray Zehr for their helpful discussions regarding this work. They also wish to thank two anonymous reviewers for their constructive comments on an earlier version of this paper.

APPENDIX A

RAMS Core

For the dry dynamical core of RAMS, the vector momentum, perturbation Exner function, and perturbation potential temperature equations are, respectively,

$$\frac{d\mathbf{v}}{dt} = \theta_0 \nabla \pi' + B\mathbf{k} - f\mathbf{k} \times \mathbf{v} + \mathbf{F_m}, \quad \text{(A1)}$$

$$\frac{\partial \pi'}{\partial t} = -\frac{c_s^2}{\rho_0 \theta_0^2} \nabla \cdot (\rho_0 \theta_0 \mathbf{v}), \quad \text{(A2)}$$

$$\frac{d\theta'}{dt} = F_\theta, \quad \text{(A3)}$$

where $\mathbf{v}$ is the vector wind, π' is the perturbation Exner function defined as the difference between the Exner function $\pi = c_p(p/p_0)^\kappa$ and the reference state Exner function π_0, $B = g\theta'/\theta_0$ is the buoyancy, and θ' is the perturbation potential temperature. Here ρ_0, θ_0, and p_0 are the reference state density, potential temperature, and pressure, respectively, and c_s is the adiabatic speed of sound. Subgrid-scale processes are represented by $\mathbf{F_m}$ in the momentum equation and by F_θ in the potential temperature equation.

For the TC-in-shear simulations the RAMS model was run nonhydrostatically and compressibly (Pielke et al. 1992). Momentum was advanced using a leapfrog scheme, while scalars were advanced using a forward scheme; in addition, both methods used second-order advection. RAMS uses the Arakawa fully staggered C grid (Arakawa and Lamb 1981). Perturbation Exner function tendencies, used to update the momentum variables, were computed using a time split scheme similar to Klemp and Wilhelmson (1978). Lateral boundaries used the Klemp–Wilhelmson condition; that is, the normal velocity component is specified at the lateral boundary and is effectively advected from the interior.

Subgrid-scale processes $\mathbf{F_m}$ were parameterized using Fickian diffusion throughout the bulk of the domain with a diffusion coefficient of 1000 $m^2\ s^{-1}$. For this value of the diffusion coefficient we observed good agreement between linear inviscid and RAMS simulations. In the vortex core the Smagorinsky deformation-based eddy viscosity (Smagorinsky 1963) was activated if values exceeded the minimum Fickian value. In all simulations shown the computed value of vertical diffusion was zero. In the simulation with 12 m s^{-1} (10

km)$^{-1}$ ambient vertical shear the vertical diffusion was nonzero in localized regions where the local vertical shear of the vortex winds was large.

REFERENCES

Arakawa, A., and V. R. Lamb, 1981: A potential enstrophy and energy conserving scheme for the shallow water equations. *Mon. Wea. Rev.*, **109,** 18–36.

Bassom, A. P., and A. D. Gilbert, 1998: The spiral wind-up of vorticity in an inviscid planar vortex. *J. Fluid Mech.,* **371,** 109–140.

Bender, M. A., 1997: The effect of relative flow on the asymmetric structure in the interior of hurricanes. *J. Atmos. Sci.,* **54,** 703–724.

Black, M. L., J. F. Gamache, F. D. Marks, C. E. Samsury, and H. E. Willoughby, 2002: Eastern Pacific Hurricanes Jimena of 1991 and Olivia of 1994: The effect of vertical shear on structure and intensity. *Mon. Wea. Rev.,* **130,** 2291–2312.

Case, K. M., 1960: Stability of inviscid plane Couette flow. *Phys. Fluids,* **3,** 143–148.

Corbosiero, K. L., and J. Molinari, 2003: The relationship between storm motion, vertical wind shear, and convective asymmetries in tropical cyclones. *J. Atmos. Sci.,* **60,** 366–376.

Davis, C. A., and L. F. Bosart, 2001: Numerical simulations of the genesis of Hurricane Diana (1984). Part I: Control simulation. *Mon. Wea. Rev.,* **129,** 1859–1881.

DeMaria, M., 1996: The effect of vertical shear on tropical cyclone intensity change. *J. Atmos. Sci.,* **53,** 2076–2087.

——, and J. Kaplan, 1999: An updated Statistical Hurricane Intensity Prediction Scheme (SHIPS) for the Atlantic and eastern North Pacific basins. *Wea. Forecasting,* **14,** 326–337.

Flatau, M., and D. E. Stevens, 1989: Barotropic and inertial instabilities in the hurricane outflow layer. *Geophys. Astrophys. Fluid Dyn.,* **47,** 1–18.

——, W. H. Schubert, and D. E. Stevens, 1994: The role of baroclinic processes in tropical cyclone motion: The influence of vertical tilt. *J. Atmos. Sci.,* **51,** 2589–2601.

Frank, W. M., and E. A. Ritchie, 1999: Effects of environmental flow upon tropical cyclone structure. *Mon. Wea. Rev.,* **127,** 2044–2061.

——, and ——, 2001: Effects of vertical wind shear on the intensity and structure of numerically simulated hurricanes. *Mon. Wea. Rev.,* **129,** 2249–2269.

Gent, P. R., and J. C. McWilliams, 1986: The instability of barotropic circular vortices. *Geophys. Astrophys. Fluid Dyn.,* **35,** 209–233.

Gray, W. M., 1968: Global view of the origin of tropical disturbances and storms. *Mon. Wea. Rev.,* **96,** 669–700.

Hawkins, H. F., and D. T. Rubsam, 1968: Hurricane Hilda, 1964: II, The structure and budgets of the hurricane on October 1, 1964. *Mon. Wea. Rev.,* **96,** 617–636.

Hoskins, B. J., and F. P. Bretherton, 1972: Atmospheric frontogenesis models: Mathematical formulation and solution. *J. Atmos. Sci.,* **29,** 11–37.

Jones, S. C., 1995: The evolution of vortices in vertical shear: Initially barotropic vortices. *Quart. J. Roy. Meteor. Soc.,* **121,** 821–851.

——, 2000a: The evolution of vortices in vertical shear. II: Large-scale asymmetries. *Quart. J. Roy. Meteor. Soc.,* **126,** 3137–3159.

——, 2000b: The evolution of vortices in vertical shear. III: Baroclinic vortices. *Quart. J. Roy. Meteor. Soc.,* **126,** 3161–3185.

Klemp, J. B., and R. B. Wilhelmson, 1978: The simulation of three-dimensional convective storm dynamics. *J. Atmos. Sci.,* **35,** 1070–1096.

Kossin, J. P., and M. D. Eastin, 2001: Two distinct regimes in the kinematic and thermodynamic structure of the hurricane eye and eyewall. *J. Atmos. Sci.,* **58,** 1079–1090.

Kurihara, Y., R. E. Tuleya, and M. A. Bender, 1998: The GFDL hurricane prediction system and its performance in the 1995 hurricane season. *Mon. Wea. Rev.*, **126,** 1306–1322.

Lamb, H., 1932: *Hydrodynamics.* 6th ed. Dover, 732 pp.

Marks, F. D., R. A. Houze, and J. Gamache, 1992: Dual-aircraft investigation of the inner core of Hurricane Norbert: Part I: Kinematic structure. *J. Atmos. Sci.,* **49,** 919–942.

McWilliams, J. C., L. P. Graves, and M. T. Montgomery, 2003: A formal theory for vortex Rossby waves and vortex evolution. *Geophys. Astrophys. Fluid Dyn.,* **97,** 275–309.

Möller, J. D., and M. T. Montgomery, 1999: Vortex Rossby waves and hurricane intensification in a barotropic model. *J. Atmos. Sci.,* **56,** 1674–1687.

——, and ——, 2000: Tropical cyclone evolution via potential vorticity anomalies in a three-dimensional balance model. *J. Atmos. Sci.,* **57,** 3366–3387.

Montgomery, M. T., and R. Kallenbach, 1997: A theory for vortex Rossby-waves and its application to spiral bands and intensity changes in hurricanes. *Quart. J. Roy. Meteor. Soc.,* **123,** 435–465.

——, and C. Lu, 1997: Free waves on barotropic vortices. Part I: Eigenmode structure. *J. Atmos. Sci.,* **54,** 1868–1885.

——, and J. Enagonio, 1998: Tropical cyclogenesis via convectively forced vortex Rossby waves in a three-dimensional quasigeostrophic model. *J. Atmos. Sci.,* **55,** 3176–3207.

——, and J. L. Franklin, 1998: An assessment of the balance approximation in hurricanes. *J. Atmos. Sci.,* **55,** 2193–2200.

——, J. D. Möller, and C. T. Nicklas, 1999: Linear and nonlinear vortex motion in an asymmetric balance shallow water model. *J. Atmos. Sci.,* **56,** 749–768.

Nolan, D. S., M. T. Montgomery, and L. D. Grasso, 2001: The wavenumber-one instability and trochoidal motion of hurricane-like vortices. *J. Atmos. Sci.,* **58,** 3243–3270.

Ooyama, K. V., 1969: Numerical simulation of the life cycle of tropical cyclones. *J. Atmos. Sci.,* **26,** 3–40.

Pearce, R. P., 1993: A critical review of progress in tropical cyclone physics including experimentation with numerical models. *Tropical Cyclone Disasters,* Peking University Press, 588 pp.

Pielke, R. A., and Coauthors, 1992: A comprehensive meteorological modeling system—RAMS. *Meteor. Atmos. Phys.,* **49,** 69–91.

Reasor, P. D., 2000: Horizontal vorticity redistribution and vortex alignment in developing and mature tropical cyclones. Ph.D. dissertation, Colorado State University, 166 pp. [Available from Dept. of Atmospheric Science, Colorado State University, Fort Collins, CO 80523.]

——, and M. T. Montgomery, 2001: Three-dimensional alignment and corotation of weak, TC-like vortices via linear vortex Rossby waves. *J. Atmos. Sci.,* **58,** 2306–2330.

——, ——, F. D. Marks Jr., and J. F. Gamache, 2000: Low-wavenumber structure and evolution of the hurricane inner core observed by airborne dual-Doppler radar. *Mon. Wea. Rev.,* **128,** 1653–1680.

Riehl, H., 1963: Some relations between wind and thermal structure of steady state hurricanes. *J. Atmos. Sci.,* **20,** 276–287.

Rivest, C., and B. F. Farrell, 1992: Upper-tropospheric synoptic-scale waves. Part II: Maintenance and excitation of quasi modes. *J. Atmos. Sci.,* **49,** 2120–2138.

Rotunno, R., and K. A. Emanuel, 1987: An air–sea interaction theory for tropical cyclones. Part II: Evolutionary study using a nonhydrostatic axisymmetric numerical model. *J. Atmos. Sci.,* **44,** 542–561.

Schecter, D. A., and M. T. Montgomery, 2003: On the symmetrization rate of an intense geophysical vortex. *Dyn. Atmos. Oceans,* **37,** 55–88.

——, D. H. E. Dubin, A. C. Cass, C. F. Driscoll, I. M. Lansky, and T. M. O'Neil, 2000: Inviscid damping of asymmetries on a two-dimensional vortex. *Phys. Fluids,* **12,** 2397–2412.

——, M. T. Montgomery, and P. D. Reasor, 2002: A theory for the vertical alignment of a quasigeostrophic vortex. *J. Atmos. Sci.,* **59,** 150–168.

Shapiro, L. J., and H. E. Willoughby, 1982: The response of balanced hurricanes to local sources of heat and momentum. *J. Atmos. Sci.,* **39,** 378–394.

——, and M. T. Montgomery, 1993: A three-dimensional balance theory for rapidly rotating vortices. *J. Atmos. Sci.*, **50,** 3322–3335.

Smagorinsky, J., 1963: General circulation experiments with the primitive equations. I: The basic experiment. *Mon. Wea. Rev.*, **91,** 99–164.

Smith, R. K., W. Ulrich, and G. Sneddon, 2000: On the dynamics of hurricane-like vortices in vertical shear flows. *Quart. J. Roy. Meteor. Soc.*, **126,** 2653–2670.

Thorpe, A. J., and R. Rotunno, 1989: Nonlinear aspects of symmetric instability. *J. Atmos. Sci.*, **46,** 1285–1299.

Vandermeirsh, F., Y. Morel, and G. Sutyrin, 2002: Resistance of a coherent vortex to a vertical shear. *J. Phys. Oceanogr.*, **32,** 3089–3100.

Wang, Y., and G. J. Holland, 1996: Tropical cyclone motion and evolution in vertical shear. *J. Atmos. Sci.*, **53,** 3313–3332.

Willoughby, H. E., 1990: Temporal changes of the primary circulation in tropical cyclones. *J. Atmos. Sci.*, **47,** 242–264.

Wu, C.-C., and K. A. Emanuel, 1993: Interaction of a baroclinic vortex with background shear: Application to hurricane movement. *J. Atmos. Sci.*, **50,** 62–76.

Zehr, R., 1992: Tropical cyclogenesis in the Western North Pacific. NOAA Tech. Rep. NESDIS 61, 181 pp.

——, 2003: Environmental vertical wind shear with Hurricane Bertha (1996). *Wea. Forecasting*, **18,** 345–356.